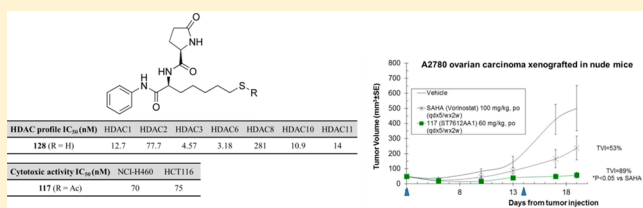


ST7612AA1, a Thioacetate- ω (γ -lactam carboxamide) Derivative Selected from a Novel Generation of Oral HDAC InhibitorsGiuseppe Giannini,^{*,†} Loredana Vesci,[†] Gianfranco Battistuzzi,[†] Davide Vignola,[†] Ferdinando M. Milazzo,[†] Mario Berardino Guglielmi,[†] Marcella Barbarino,[†] Mosè Santaniello,[†] Nicola Fantò,[†] Marco Mor,[‡] Silvia Rivara,[‡] Daniele Pala,[‡] Maurizio Taddei,[§] Claudio Pisano,^{†,||} and Walter Cabri^{†,⊥}[†]R&D Sigma-Tau Industrie Farmaceutiche Riunite SpA, Via Pontina Km 30,400, I-00040 Pomezia, Roma, Italy[‡]Dipartimento di Farmacia, Università degli Studi di Parma, Parco Area delle Scienze 27/A, I-43124 Parma, Italy[§]Dipartimento di Biotecnologie, Chimica e Farmacia, Università degli Studi di Siena, Via A. Moro 2, I-53100 Siena, Italy

S Supporting Information

ABSTRACT: A systematic study of medicinal chemistry aimed at identifying a new generation of HDAC inhibitors, through the introduction of a thiol zinc-binding group (ZBG) and of an amide-lactam in the ω -position of the polyethylene chain of the vorinostat scaffold, allowed the selection of a new class of potent pan-HDAC inhibitors (pan-HDACis). Simple, highly versatile, and efficient synthetic approaches were used to synthesize a library of these new derivatives, which were then submitted to a screening for HDAC inhibition as well as to a preliminary in vitro assessment of their antiproliferative activity. Molecular docking into HDAC crystal structures suggested a binding mode for these thiol derivatives consistent with the stereoselectivity observed upon insertion of amide-lactam substituents in the ω -position. ST7612AA1 (**117**), selected as a drug candidate for further development, showed an in vitro activity in the nanomolar range associated with a remarkable in vivo antitumor activity, highly competitive with the most potent HDAC inhibitors, currently under clinical trials. A preliminary study of PK and metabolism is also illustrated.



INTRODUCTION

Since 1964, when Allfrey, Faulkner, and Mirsky discovered the reversible acetylation of histone proteins,¹ much has been learned on their role and importance in pathophysiological conditions. Over these 50 years, therapeutic prospects for epigenetic modulation have become increasingly concrete, even if a growing body of literature is highlighting the complexity of the histone proteins that should be rather considered as a cluster of proteins. Histone deacetylase inhibitors represent one of the most advanced tools for epigenetic modulation, although a plethora of other nonhistone proteins are modulated by this class of compounds. After recent important proteomic studies,^{2–4} we can now refer to a more appropriate definition of “lysine deacetylases” instead of “histone deacetylases”. However, so far the attention has been focused mainly on histone deacetylases (HDACs), which play an important role in reversing aberrant epigenetic changes associated with cancer as well as with noncancer diseases (i.e., neurological and inflammatory pathologies). Overexpression of these enzymes has been shown in several types of cancer with a different behavior from isoform to isoform, hence generating the interest toward HDAC inhibitors in various oncological clinical applications. All HDAC inhibitors studied so far, including the first two FDA approved, vorinostat (**1**) and romidepsin (**2**) depicted in Figure 1, work by inhibiting not only the

deacetylation of histone proteins but also, and perhaps primarily, of a large number of other nonhistone (cytoplasmic and nuclear) proteins. For this reason much still remains to be elucidated, and impressive opportunities await pharmaceutical companies and clinicians committed to finding novel therapeutic solutions.

Compounds **1** (SAHA, vorinostat, Zolinza) and **2** (depsipeptide; FK-228, Istodax) are the two HDAC inhibitors currently used in the clinical practice. Both compounds were licensed by the FDA, in 2006 and 2009, respectively, for the treatment of the rare cancer, cutaneous T-cell lymphoma. In 2011, **2** was approved for an additional indication, the peripheral T-cell lymphoma.

In addition to these two first-in-class compounds, more than 20 new HDAC inhibitors are currently under preclinical and clinical investigation against different cancers as well as for several other novel therapeutic indications. For an overview of this topic, the reader is encouraged to consult a recent review published by some of us⁵ and other interesting reviews covering this area.^{6–9}

Human HDACs are divided into four classes (I–IV) based on their homology to yeast HDACs, their subcellular

Received: May 29, 2014

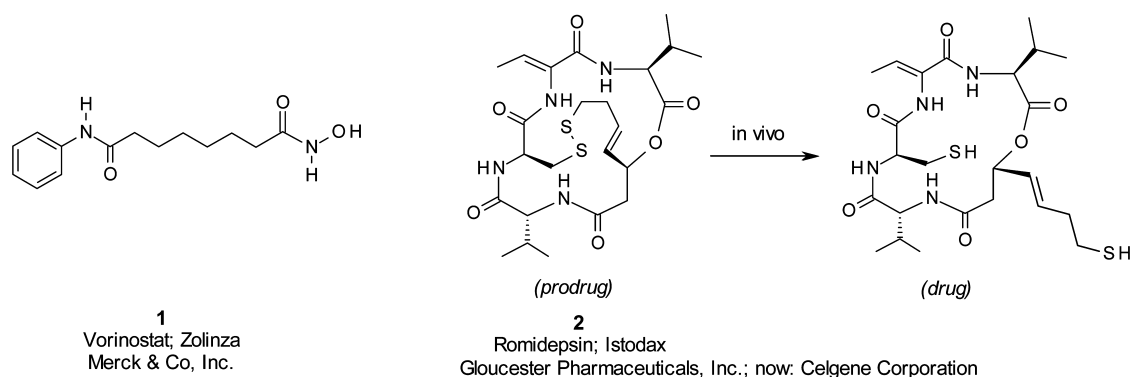


Figure 1. Chemical structure of the two FDA approved HDAC inhibitors. Romidepsin (2) is a prodrug, with a disulfide bridge reduced by glutathione upon uptake into the cell, allowing the release of the drug (thiol free).

localization, and their enzymatic activities. Classes I–II and IV are Zn^{2+} -dependent amidohydrolases, while class III enzymes, also called sirtuins, greatly differ from the previous ones because they use NAD as a cofactor. So far, 11 HDAC isoforms have been identified in humans belonging to the Zn^{2+} -dependent group. Class I HDAC family consists of HDAC1, 2, 3, and 8, primarily detected in the nucleus, and with isoform 8 also found in the cytoplasm. These are small proteins expressed ubiquitously in various human cell types and tissues displaying high enzymatic activity toward histone and other protein substrates with a primary role in controlling and regulating cell survival, proliferation, and differentiation. Class II HDAC family, which in turn is further divided into two subclasses, class IIa (HDAC4, 5, 7, and 9) and class IIb (HDAC6 and 10), encompasses larger proteins expressed in a limited number of cell types. They either shuttle between the nucleus and cytoplasm (i.e., class IIa) or are mainly located within the cytoplasm (i.e., class IIb), with more tissue-specific regulatory function than class I HDACs. HDAC11 is the sole isoform of class IV, the least investigated so far, although it has recently been reported that a selective depletion of this isoform, overexpressed in several carcinomas, is sufficient to cause cell death and to inhibit metabolic activity in various cancer cell lines.¹⁰

Since 1996, when the first HDAC inhibitor, trapoxin,¹¹ was identified, much progress has been made in the knowledge of the biology and the structural aspects of the different HDAC isoforms. Moreover, new assays have been set up, allowing the evaluation of the selectivity profile of the newly synthesized inhibitors. Nevertheless, the scientific community has not yet been able to prove the advantage, in terms, for example, of increased efficacy and/or decreased adverse events of selective HDAC inhibitors (toward a single-isoform or single-class) over pan-inhibitors, also because of the expanding interest of these inhibitors in other therapeutic applications, different from cancer.¹² However, an increasingly greater characterization of individual tumors to the overexpression of single isoforms or class of HDACs is available.^{5,13} But, so far, these observations have not been translated into any therapeutic advantage, rendering selective inhibitors superior to pan-inhibitors.

We started our project with reference to the widely accepted pharmacophore model for HDAC inhibitors, represented by a zinc-binding group (ZBG) able to complex the Zn^{2+} ion at the bottom of the catalytic cavity, opposite to a capping group (CAP), able to interact with the rim of the catalytic tunnel of the enzyme, and a hydrophobic linker connecting the two parts.

A kink atom completes the model, as connection unit (CU) between linker and CAP (Figure 2).⁵

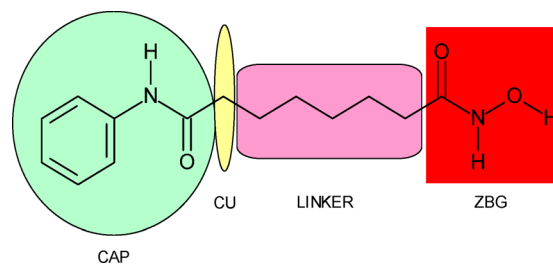


Figure 2. Pharmacophore model for HDAC inhibitors applied to the structure of compound 1.

Our interest was mainly focused on two elements of this model, the ZBG and CU. Numerous studies have been made to identify new groups, metabolically stable, able to chelate the Zn^{2+} ion. To date, the ZBGs introduced in the most preclinically and clinically advanced HDAC inhibitors are carboxylic acid, a weak Zn-chelating group present in compounds active in the millimolar range (i.e., valproic acid), hydroxamic acid, a powerful Zn-chelating group found in compounds active in the range between submicromolar to one-digit nanomolar concentrations (i.e., vorinostat, panobinostat, belinostat, etc.), and benzamide (i.e., entinostat, mocetinostat, tacedinaline, etc.). Only one natural derivative with a thiol residue, masked as a disulfide moiety undergoing in vivo reduction (2), has successfully passed clinical trials getting to the FDA approval.

A recent paper by Grassadonia et al.¹⁴ analyzed the role of hydroxamate-based HDAC inhibitors, highlighting that these drugs seem to be more active in hematological malignancies than in solid tumors. A possible explanation might involve the pharmacokinetic profile of hydroxamate-based HDAC inhibitors. Therefore, the availability of novel inhibitors with nonhydroxamate ZBGs represents now a highly desirable condition.¹⁵ The thiol group has been successfully introduced in drugs like the antidiarrheal Racecadotril (Acetorphan)¹⁶ and the antihypertensive angiotensin-converting enzyme inhibitor Captopril (Capoten).¹⁷ It has been also widely investigated in HDAC inhibitors,^{18–20} including cyclic tetrapeptides,²¹ and has been found to be a potent Zn-chelating group. In fact, replacement of the hydroxamate portion of 1 with a thiol group provided compounds with comparable HDAC inhibitory potency and cancer cell growth inhibition for their S-modified

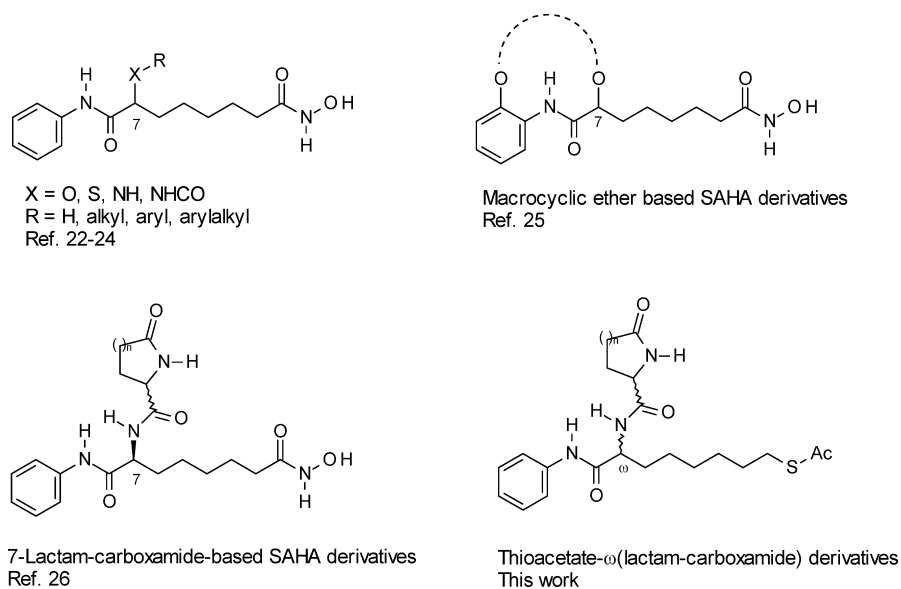
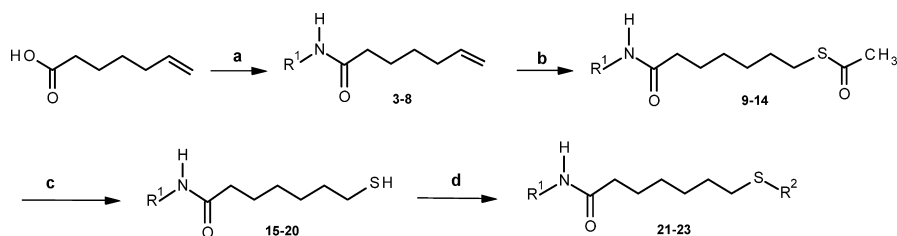


Figure 3. Examples of ω -substituents on the aliphatic chain of suberoylanilide hydroxamic acid (**1**) and ω -substituted thioacetates described in this work.

Scheme 1. Synthesis of Linear Reference Compounds 9–23^a



^aReagents and conditions: (a) R^1NH_2 , PyBOP, NEt_3 , DMF, and DCM, RT; (b) AcSH, AIBN, dioxane, 75 °C; (c) CH_3SNa , MeOH, RT; (d) R^2Cl , Et_3N , DCM, RT.

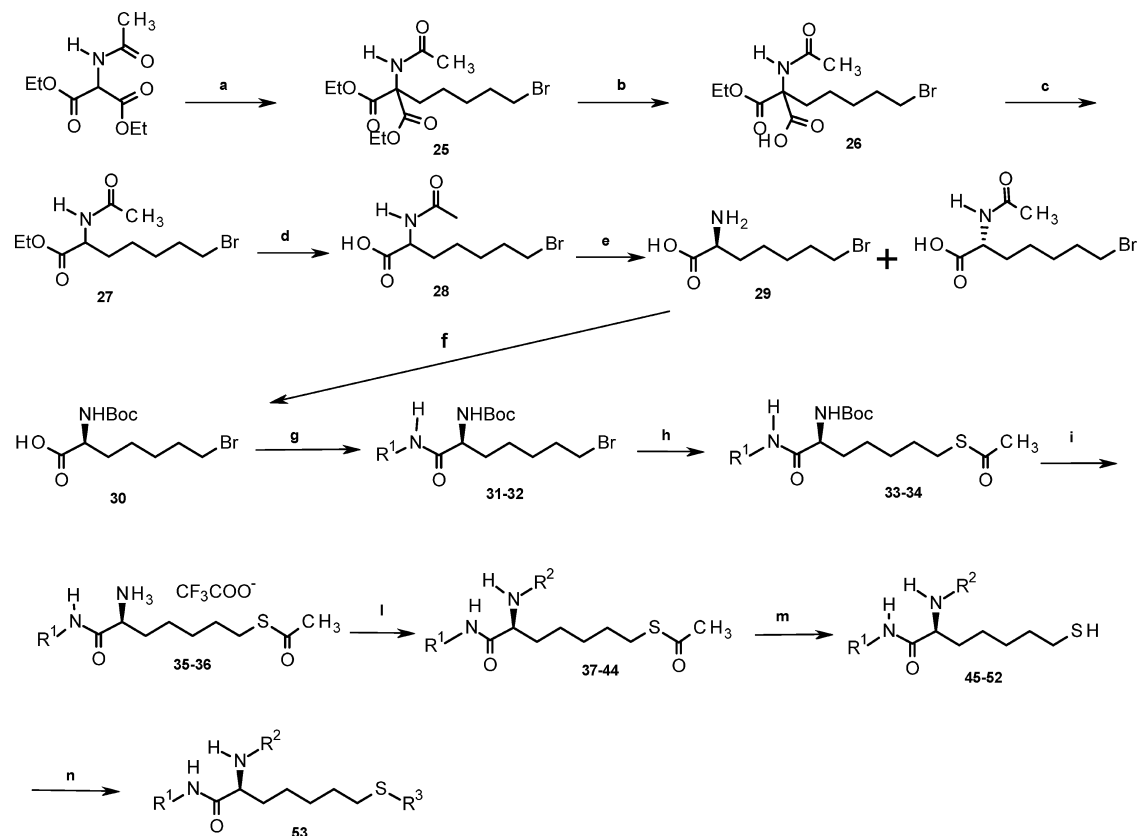
prodrugs. Until now, no synthetic thiol derivative has been included in a clinical trial because of the thiol reactivity and too easy capability of oxidation. However, given the interesting clinical profile of **2**, we wanted to further explore the potential of the thiol group in a new class of synthetic HDAC inhibitors.

A second point where we focused our interest was the kink atom or connecting unit (CU, Figure 2). The introduction of substituents on the methylene chain, in ω -position, has been extensively studied, leading to more potent and/or more selective derivatives. The first attempts were made by Breslow and co-workers, with a series of 7-substituted ethers, amines, and amide derivatives of **1** with excellent inhibitory activities.²² Efforts in the same direction were made also in our laboratory, studying different 7-alkoxy derivatives alone^{23,24} or inserted in a macrocyclic fraction,²⁵ and more recently, introducing lactam-carboxamide substituents (Figure 3).²⁶ In all these examples, the introduction of substituents on the methylene chain showed an enhancement of the activity compared to the parent compound, leading to a strong inhibition of different HDAC isoforms associated with a high cytotoxic potency against selected tumor cell lines.

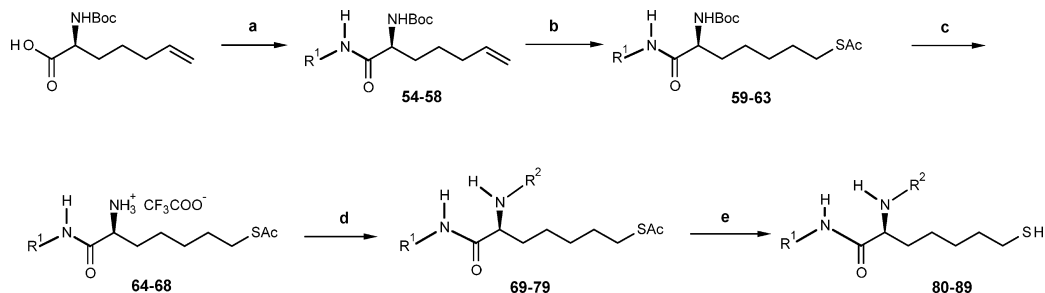
In this article, we present new HDAC inhibitors based on a protected thiol group replacing the hydroxamate ZBG of **1**, containing lactam carboxamide substituents in ω -position of the methylene chain (Figure 3). β -, γ -, and δ -lactams were inserted in ω -position of the carboxamide fragment, and the effect of different configurations of both C7 carbon atom and

lactam stereocenters was evaluated. The importance of the phenyl ring in the CAP region was also investigated, preparing benzyl, phenethyl, and cyclopentyl derivatives. An enhancement of HDAC inhibitory activity was observed not only versus the parent compounds, lacking substituents on the methylene chain, but also toward the corresponding hydroxamic acid derivatives. Docking studies into HDAC crystal structures gave results consistent with structure–activity relationships (SAR). Docking poses for different stereoisomers of lactam carboxamide inhibitors into HDAC3 correctly predicted the highest inhibitory potency observed with ω -(*S*)-derivatives. Moreover, docking solutions provided an explanation for the highest inhibitory activity on HDAC8 found with benzyl and phenethyl derivatives compared to their phenyl analogues.

We report here multiple chemical approaches for the preparation of these lactam carboxamide inhibitors and their characterization as HDAC inhibitors. The thioacetyl derivative ST7612AA1 (**117**) showed a high cytotoxic activity on NCI-H460 and HCT116 cell lines and a high inhibitory potency against tubulin and histone H4 acetylation in cellular assays. This compound was also investigated for its metabolic stability and antitumor activity against two human solid tumors, a colon carcinoma HCT116 and an ovarian A2780 tumor xenograft models. As a potent HDAC inhibitor, promising results in terms of in vitro profile, formulation, metabolic stability, cell permeability, and in vivo activity are herein described.

Scheme 2. Synthesis of Thioacetates 37–44, Thiols 45–52, and the Derivative 53^a

^aReagents and conditions: (a) (1) EtOH, EtONa, reflux, 30 min, (2) Br(CH₂)₅Br, reflux, 3 h; (b) NaOH aq, EtOH, 0 °C, 5 h; (c) toluene, reflux, 4 h; (d) NaOH aq, EtOH, 0 °C, 4 h; (e) aminoacylase, H₂O, pH 7, CoCl₂·6H₂O, 38 °C, 24 h; (f) (Boc)₂O, Et₃N, THF, H₂O, rt, 20 h; (g) R¹NH₂, EDCl, HOBT·H₂O, THF, RT; (h) KSac, EtOH, RT; (i) CF₃COOH, CH₂Cl₂, RT, 5 h; (l) R²COOH, DMF, PyBOP, DIPEA, rt, 20 h; (m) 2N NaOH, EtOH, RT; (n) R³Cl, Et₃N, DCM, RT.

Scheme 3. Synthesis of Thioacetates 69–79 and Thiols 80–89^a

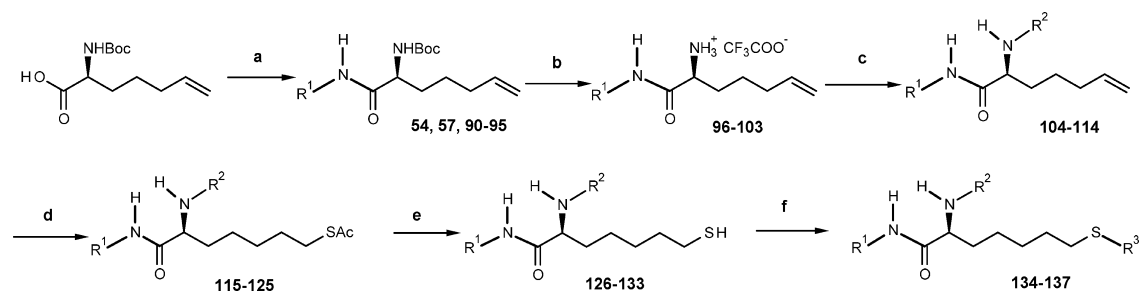
^aReagents and conditions: (a) R¹NH₂, PyBOP, NEt₃, DMF and DCM, RT; (b) AcSH, AIBN, dioxane, 75 °C; (c) TFA, DCM, 0 °C to RT; (d) R²COOH, PyBOP, NEt₃, DMF and DCM, RT; (e) CH₃SNa, MeOH, RT, 0.1 M HCl.

CHEMISTRY

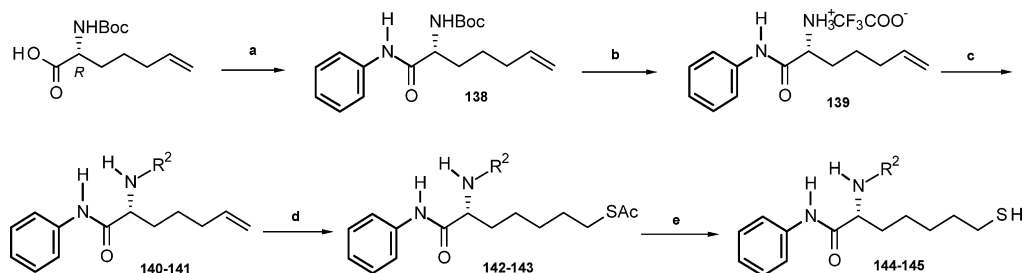
Syntheses of thiol HDAC inhibitors were carried out as outlined in Schemes 1–5. The route for synthesis of compounds 9–23 is described in Scheme 1. Condensation of hept-6-enoic acid with appropriate amines afforded amides 3–8, which in their turn were treated with thioacetic acid and AIBN in dioxane to yield the desired thioesters 9–14. Compounds 15–20 were synthesized by hydrolysis of thioester with sodium thiomethoxide in MeOH under dry nitrogen atmosphere. It is noteworthy that the classical procedure of hydrolysis with NaOH/H₂O, reflux (or with KOH, K₂CO₃, NaOMe),²⁷ led to a significant proportion of the oxidized

product (S–S). Condensation of compound 15 with appropriate chlorides (i.e., ethyl chloroformate, isobutyryl chloride, and (2*R*)-2-amino-3-methyl-butanoyl chloride) afforded thioesters 21–23. Compound 24 is derived from oxidation of thiol 9 as side product after hydrolysis.

The remaining molecules were prepared following four different synthetic approaches. Compounds 37–53, including the three reference ones 44, 52, and 53, were synthesized following the synthetic method described in the literature^{20,28} except for the Boc protection of the amino acid 29 (Scheme 2). As an alternative (Scheme 3), commercially available (*S*)-2-*tert*-butoxycarbonylamino-hept-6-enoic acid was coupled with the proper aromatic amines to obtain compounds 54–58, then

Scheme 4. Synthesis of Thioacetates 115–125, Thiols 126–133, and Thio-derivatives 134–137^a

^aReagents and conditions: (a) R^1NH_2 , PyBOP, NEt_3 , DMF and DCM, RT; (b) TFA, DCM, 0 °C to RT; (c) R^2COOH , PyBOP, NEt_3 , DMF and DCM, RT; (d) AcSH, AIBN, dioxane, 75 °C; (e) CH_3SNa , MeOH, RT, 0.1 M HCl; (f) R^3Cl , Et_3N , DCM, RT.

Scheme 5. Synthesis of Derivatives with *R* Chirality in ω -Position^a

^aReagents and conditions: (a) $PhNH_2$, PyBOP, NEt_3 , DMF and DCM, RT; (b) TFA, DCM, 0 °C to RT; (c) R_2COOH , PyBOP, NEt_3 , DMF and DCM, RT; (d) AcSH, AIBN, dioxane, 75 °C; (e) CH_3SNa , MeOH, RT, 0.1 M HCl.

thioacetylation was achieved by AIBN with thioacetic acid followed by Boc removal with TFA. The obtained thioesters **64–68** were reacted with the proper lactam carboxylic acid to afford compounds **69–79** that were subsequently hydrolyzed with sodium thiomethoxide in MeOH to obtain thiols **80–89**. Thioacetate derivatives **115–125** and thiols **126–133** were synthesized according to Scheme 4, similar to the above synthesis except for the coupling with the proper lactam carboxylic acid carried out before the thioacetylation with AIBN and thioacetic acid. Condensation of compounds **127** and **128** with the appropriate acid or ethylchloroformate afforded thioesters **134–136**. Dithio compound **137** was obtained as the side-product from the hydrolysis step of **116** to give **127**. Compounds **143–145** were synthesized according to Scheme 5. Commercially available (*R*)-2-*tert*-butoxycarbonylaminohept-6-enoic acid was coupled with aniline to obtain compound **138**, then Boc removal with TFA, followed by coupling with the proper lactam carboxylic acid to afford compounds **140–141**. Then thioacetylation was achieved by AIBN with thioacetic acid. The obtained thioesters **142–143** were hydrolyzed with sodium thiomethoxide in MeOH to obtain thiols **144–145**. Recently, a different synthetic approach to obtain thiol derivatives analogues to ours has been reported.²⁹

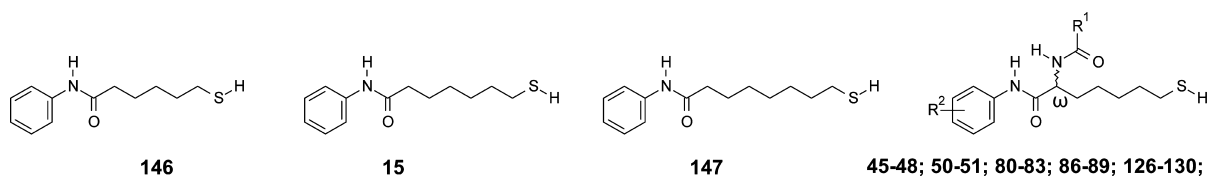
RESULTS AND DISCUSSION

We systematically investigated several ω -lactam-carboxamide thiols for their *in vitro* inhibitory activity on different HDAC isoforms and for their antiproliferative activity on tumor cell lines. In Table 1, the inhibitory activities on class I (1–3, 8), IIb (6, 10), and IV (11) HDAC isoforms are reported. Class IIa (4, 5, 7, 9) enzymes were not considered for structure–activity relationships evaluation and compound optimization. In fact, it is known that class IIa enzymes are very inefficient on histone substrates and exert a transcriptional repression function mainly

through their ability to directly inactivate specific transcription factors.^{30,31} Indeed, when tested on class IIa isoforms, our thiol inhibitors usually gave IC_{50} values in the micromolar range, with no apparent correlation with their structure. The inhibitory activities of the newly synthesized compounds on class IIa isoforms are reported in Supporting Information Table S2.

We started our investigation on thiol derivatives of compound **1** by verifying the optimal length of the methylene chain connecting the amide function to the terminal thiol group. In fact, HDAC activity of compounds with different chain lengths had been tested only on HeLa nuclear extracts¹⁹ and, in the literature, data on the different isoforms have not been reported so far. Compounds **15** and **147** with 6 and 7 methylene units, respectively, were generally more potent than the 5 methylene-derivative **146**. We decided to focus on the 6 methylene chain (also present in reference compound **1**) given the superior activity of its acetyl prodrug in *in vitro* antiproliferative studies on NCI-H460 cell line ($IC_{50} = 14.8 \mu M$ measured for **15** and $IC_{50} > 30 \mu M$ for **147**).

The first ω -lactam carboxamide substituent to be evaluated was the six-membered one, for which the importance of stereochemistry of both the lactam ring and the ω position of the amide chain was investigated. We found that the configuration of the stereocenter in ω position is crucial for good inhibitory potency, while configuration of the lactam substituent is irrelevant. In fact, compound **144** with ω -(*R*) chirality was practically inactive on all HDAC isoforms, while its enantiomer **126** and the diastereoisomer **127**, having both *S* configuration in the ω position, had comparable and good inhibitory potencies. With the lactam carboxamide in the ω position having the most favorable *S* configuration, the substituent improved inhibitory potency on all isoforms compared to the unsubstituted **15**. This effect reflects the

Table 1. In Vitro Inhibitory Activity (IC₅₀) of Thiol Derivatives Against Isoforms HDAC1–3, 6, 8, 10, 11^a

Compd.	ST code number	ω -chirality	R ¹	R ²	IC ₅₀ (nM)						
					HDAC1	HDAC2	HDAC3	HDAC6	HDAC8	HDAC10	HDAC11
1					258	921	350	28	243	456	362
15	ST7660				288	1300	201	19	1070	270	262
146	ST7775				791	2220	725	67	1360	1220	659
147	ST7783				294	754	110	70	1120	252	133
127	ST7538	S		H	15	67	10	6	416	11	6
126	ST7896	S		H	10	34	6	5	107	32	10
144	ST8023	R		H	<i>b</i>	<i>b</i>	17100	9380	<i>b</i>	<i>b</i>	14200
82	ST8013	S		H	11	70	7	3	202	6	5
51	ST7539	S		H	7	28	3	1	62	9	9
50	ST7540	S		H	12	48	5	1	122	11	15
129	ST8001	S		<i>m</i> -CH ₃	2	15	1	1	135	1	1
130	ST8000	S		<i>p</i> -CH ₃	8	60	3	2	360	4	3
81	ST8077	S		H	24	33	13	1	59	15	30
128	ST7464	S		H	13	78	5	3	281	11	14
145	ST8085	R		H	101	171	138	21	8100	40	102
83	ST8080	S		H	58	103	49	5	545	116	67
86	ST8084	S		<i>m</i> -CH ₃	5	13	4	1	106	5	62
87	ST8083	S		<i>m</i> -CH ₃	4	14	3	2	106	4	5
88	ST8082	S		<i>m</i> -CH ₃	3	5	5	1	99	2	12

Table 1. continued

Compd.	ST code number	ω -chirality	R ¹	R ²	IC ₅₀ (nM)						
					HDAC1	HDAC2	HDAC3	HDAC6	HDAC8	HDAC10	HDAC11
89	ST8081	S		<i>m</i> -CF ₃	5	12	11	5	316	7	44
45	ST7541	S		H	7	37	2	4	40	5	4
46	ST7542	S		H	53	2230	55	160	2040	7	12
47	ST7543	S		H	32	168	9	4	310	14	13
48	ST7544	S		H	74	1900	72	35	2570	14	24
80	ST7897	S		H	8	68	8	2	61	9	10

^aValues are the means of a minimum of three experiments. ^bNo inhibition at concentration <50 μ M.

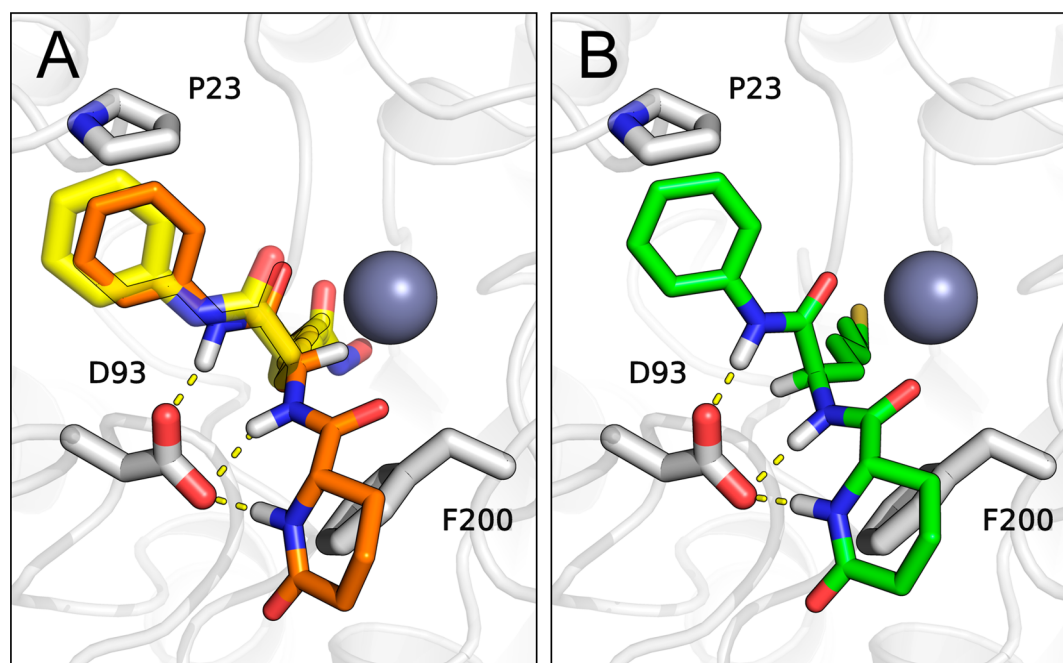
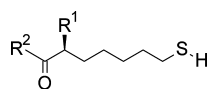


Figure 4. Docking solutions for ω -(*S*)-127 (orange carbons) and its diastereoisomer ω -(*R*)-144 (green carbons) into HDAC3 active site. Compound 1 (yellow carbons) cocrystallized with HDAC2 (PDB 4LHZ) is depicted for comparison.

results already reported for lactam carboxamide derivatives of 1.²⁶ On the other hand, the increase of inhibitory potency given by the lactam carboxamide substituent was greater for these thiol derivatives than for hydroxamic acid counterparts. The highest potency of the (*S*)- ω -amide derivative was consistent with the presence of the same configuration within the natural peptide substrate, and it can be rationalized on the basis of the putative binding mode. To evaluate the accommodation of lactam carboxamide derivatives into the enzyme active site, HDAC3 obtained from the crystal structure of its complex with an acetate product was selected as a model structure and it was used for docking studies. The docking poses found for compounds 127 and 144 are represented in Figure 4.

Compound 127 was strongly bound to Asp93 in the rim of the active site, while the thiol group was deeply inserted into the active site and coordinated the zinc ion. A similar binding mode was also observed for reference compound 1 in its crystallized complex with HDAC (Figure 4, left panel). The lactam ring was exposed to the solvent and was involved in limited interactions with amino acids in the rim of the binding site. This could explain the lack of stereoselectivity observed for the lactam stereocenter and the limited effect on potency of lactam ring modifications (ring contraction, opening, substitution, i.e., see next SAR discussion). Compound 144 showed the same polar interactions as compound 127 even if, given the opposite stereochemistry, its ω -hydrogen atom

Table 2. In Vitro Inhibitory Activity (IC₅₀) of Thiol Derivatives with Modified CAP Group Against Isoforms HDAC1–3, 6, 8, 10, 11^a

Compd.	ST code number	R ¹	R ²	IC ₅₀ (nM)						
				HDAC1	HDAC2	HDAC3	HDAC6	HDAC8	HDAC10	HDAC11
19	ST7784	H		865	6640	897	87	2330	1170	776
133	ST7786			160	454	98	6	450	189	89
52 ^b	ST7306			c	c	c	1120	44000	5210	30700
18	ST7881	H		5960	19400	2710	5300	373	6290	2070
131	ST7893			386	1770	475	139	23	310	140
17	ST7819	H		3160	14000	2950	1770	904	2990	1840
132	ST7894			504	2540	495	83	9	658	293
20	ST7807	H		3210	10700	2600	2710	246	3930	1870
84	ST7899			92	601	122	15	17	81	82
16	ST7817	H		1750	c	35800	c	c	2930	949
85	ST7900			2900	c	6330	582	2230	6000	293

^aValues are the means of a minimum of three experiments. ^bReference 20. ^cNo inhibition at concentration <50 μM.

points toward the carboxylic group of Asp93 (Figure 4, right panel). The binding modes of compounds 127 and 144 resembled those of a P53-derived diacetylated peptide substrate and of a peptide inhibitor with *R* stereochemistry,³² respectively, crystallized into HDAC8 (Supporting Information Figure S1). The opposite stereochemistry of the ω-carbon atom had a strong impact on the stability of the corresponding complexes, as evaluated by molecular dynamics (MD) simulations into an explicit water box. Compound 127 remained stably bound to the active site amino acids during the 20 ns long MD simulations, while compound 144 lost its interactions with HDAC residues in the first steps of the simulation (Supporting Information Table S3).

Modifications of the lactam ring, such as *N*-methylation (82) and inversion of the lactam function (50, 51), did not significantly affect the inhibitory potency of the compounds compared to the reference 127. On the other hand, the presence of a methyl group on the phenyl ring had a favorable effect, leading to an increase of inhibitory potency on all isoforms when inserted in *para*-position (130) and, particularly, in *meta*-position (129). The positive effect of a *meta*-methyl had already been observed for hydroxamate-based inhibitors on total HDAC activity in Caco-2 colon cancer cells, meanwhile *para*-methyl analogues demonstrated slightly reduced inhibitory activity.³³

Ring contraction to γ-lactam (81, 128) afforded compounds with HDAC inhibitory potency comparable to those with larger δ-lactams, with similar SARs. Indeed, the presence of an (*R*)-ω-amide stereocenter significantly lowered the potency (145), even if to a lower extent than in the δ-lactam series. Methylation of the lactam nitrogen on the 7*S*/2'*R* derivative led to a modest reduction of inhibitory potency on all HDAC isoforms (83). As observed for δ-lactam derivatives, the presence of a methyl group in *meta*-position of the phenyl ring (86, 87, 88) led to an increase of inhibitory potency, particularly for the 7*S*/2'*R* configuration. Replacement of the methyl substituent with a trifluoromethyl (89) did not bring any further improvement. Four γ-lactam derivatives were also prepared (45, 46, 47, 48) with inverted amide function and insertion of a phenyl substituent close to the lactam connection point. The phenyl substituent was not detrimental to the activity, particularly on lactams with 3'*S* chirality (45, 47), with the highest inhibitory potency observed with compound 45 having 7*S*/3'*S*/4'*R* stereochemistry. A further contraction of the lactam ring, the β-lactam 80, maintained good inhibitory potencies, comparable to the γ-lactam analogue 81.

An exploration of the CAP region was also done with the synthesis of different aliphatic amides (Table 2). We first evaluated the cyclopentyl ring which conferred selectivity for HDAC6 to thiol-based HDAC inhibitors.²⁰ Replacement of the

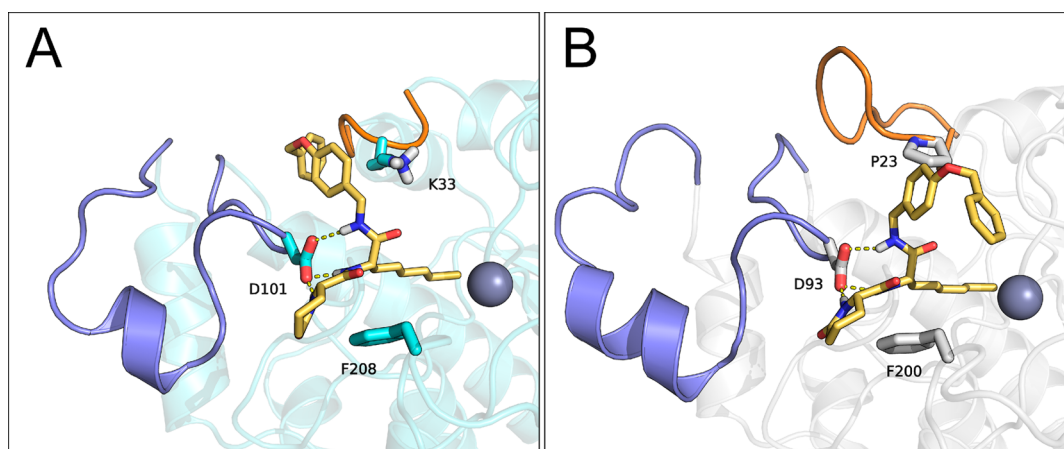


Figure 5. Docking poses of compound **132** into HDAC8 (left) and HDAC3 (right) crystal structures. Loop L1 is depicted as an orange tube and L2 in light blue.

phenyl ring with a cyclopentyl moiety (**19**) maintained the 10-fold selectivity for HDAC6 already observed for the phenyl derivative **15**. Insertion of the lactam carboxamide substituent on the cyclopentyl derivative **19** produced compound **133**, which showed improved inhibitory potency and selectivity for HDAC6. Carbamate derivative **52**, reported as an HDAC6-selective inhibitor,²⁰ in our hands gave poor results, with very limited inhibitory activity on HDAC6 isoform. An inferior potency of carbamoyl derivative **52** compared to lactam carboxamide **133** could be explained on the basis of their accommodation within the HDAC catalytic site. In fact, while docking studies for **52** showed a pose similar to that of lactam carboxamide derivatives, the carbamic oxygen of **52** was close to the carboxylic group of Asp93, exerting an unfavorable repulsive effect (Supporting Information Figure S2).

Phenylalkyl substituents were also investigated, such as *p*-trifluoromethylbenzyl (**18**, **131**), benzyloxy-benzyl (**17**, **132**), and *m*-methylphenylethyl derivatives (**20**, **84**), in which the lactam carboxamide substituent always improved the inhibitory potencies of the unsubstituted parent counterparts (as detailed in Table 2). Interestingly, these phenylalkyl derivatives showed a certain selectivity for HDAC8 compared to the other class I enzymes, while their phenyl analogue **127** had its lowest inhibitory potency on this isoform. Docking studies with compound **132** into a HDAC8 crystal structure evidenced that the benzyloxy-benzyl substituent can be inserted into a pocket lined by the N-terminal L1 loop (Figure 5). The same accommodation was not possible in the case of HDAC3. In fact, HDAC8 L1 loop is two residues shorter than that of the other class I HDACs, resulting in a wider active-site pocket with a larger surface opening and higher flexibility.³⁴ The region occupied by the benzyl fragment was very close to the secondary pocket observed in the HDAC8 crystal structure in complex with selective inhibitors.³⁴ The benzyloxy-benzyl substituent adopted a different conformation in the complex with HDAC3, being essentially solvent exposed. Finally, a tetrahydroisoquinoline, incorporating the amide nitrogen atom, was also evaluated. The poor inhibitory potencies of compounds **16** and **85** supported the need of the free amide NH group for HDAC binding and inhibition.

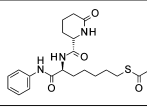
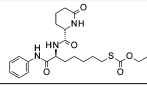
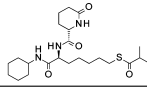
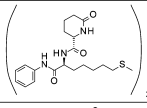
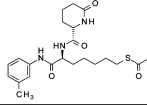
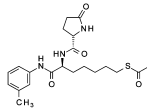
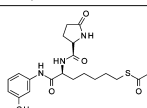
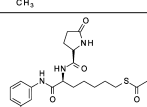
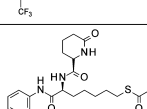
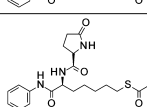
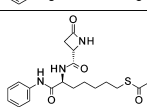
The antiproliferative activity of thiol inhibitors greatly improved when their sulfhydryl group was transiently masked as a prodrug.¹⁸ To select the most effective protective group for our thiols, we started studying the solubility and stability of

various derivatives (acetyl, thiocarbonate, isobutyryl, aminoacyl, and the dimeric oxidized form) of the linear compound **15**. The results obtained were in line with what was described in the literature and are reported in Supporting Information Table S4a. The acetyl (**9**), isobutyryl (**22**), and thiocarbonate (**21**) derivatives were soluble in H₂O (>1 mg/mL) and, with the exception of the acetyl one, even at pH = 7.4. These compounds were stable in aqueous solution at pH = 1.2 (3 h) and pH = 7.4 (24 h), contrarily to aminoacyl (**23**) and disulfide (**24**) derivatives. In addition, the acetyl and isobutyryl prodrugs tested on NCI-H460 nonsmall cell lung carcinoma (NSCLC) cell line showed IC₅₀ values in the range of 15–20 μM (Supporting Information Table S5a). The other thiol derivatives **23**, **21**, and **24** had IC₅₀ values >30 μM. A similar study was conducted on ω-functionalized compounds, and solubility and stability data for derivatives of compound **127** are reported in Supporting Information Table S4b. In this case, the isobutyryl derivative **135** was unstable, while the thiocarbonate (**136**) and the acetyl (**116**) analogues were stable. Table 3 reports the results of cytotoxicity assays for these prodrugs and for the most potent prodrugs of other inhibitors (i.e., those with IC₅₀ ≤ 0.1 μM; the complete list of cytotoxic activity data can be found in Supporting Information Tables S5a, S5b). On NCI-H460 cell line, the acetyl derivative was found to be more active than the thiocarbonate analogue (IC₅₀ 0.1 vs 0.5 μM). For this reason, the acetyl was chosen as the protecting group for prodrug preparation.

The acetyl derivatives of our thiol inhibitors showed cytotoxicity potencies on NCI-H460 cell line generally consistent with their inhibitory activity on HDAC isoforms (Tables 3 and Supporting Information Tables S5a, S5b). The highest activities were seen for meta-substituted phenyl derivatives **119**, **76**, **77**, and **79** and for unsubstituted δ-, γ-, and β-lactams **116**, **115**, **117**, and **69**. In these assay conditions, reference compound **1** was significantly less potent.

The efficacy of δ-lactam **116**, γ-lactam **117**, and β-lactam **69** acetyl prodrugs was further evaluated in a cytotoxicity assay on HCT116 colon cancer cells. Moreover, their ability to affect acetylation of tubulin and histone H4 substrates, which is mainly dependent on HDAC6 and class I HDACs, respectively, was assessed through Western Blot analysis on NCI-H460 NSCLC cells (Table 4). Cytotoxic activity on HCT116 cells was in line with that seen on NCI-H460 cells, with similar IC₅₀ values and with the highest activity observed for compounds

Table 3. In Vitro Cytotoxic Activity (IC_{50}) of Selected Lactam-Carboxamide Thiol Prodrugs on H460 Lung Cancer Cells^a

Compd.	ST code number		NCI-H460 cytotoxicity IC_{50} (μ M)
1		-	3.40
116	ST7572		0.10
136	ST7905		0.51
135	ST7904		3.70
137	ST7811		5.40
119	ST7918		0.06
76	ST8036		0.06
77	ST8035		0.04
79	ST8039		0.03
115	ST7874		0.10
117	ST7612		0.07
69	ST7876		0.05

^aValues are the means of a minimum of three experiments.

Table 4. In Vitro Cytotoxic Activity (IC_{50}) of Selected Acetyl Prodrugs on HCT116 Colon Cancer Cell Line, and Assessment (through Western Blot) of Their Inhibitory Activity on Acetylation of Tubulin and Histone H4 Target Proteins in NCI-H460 Cells^a

compd	ST code number	HCT116 cytotoxicity IC_{50} (μ M)	tubulin acetylation (WB) IC_{50} (μ M)	histone H4 acetylation (WB) IC_{50} (μ M)
116	ST7572	0.130	0.10	0.100
117	ST7612	0.075	0.20	0.005
69	ST7876	0.086	0.05	0.031

^aValues are the means of a minimum of two experiments.

117 and 69. Compound 117 showed its highest inhibitory activity on acetylation of histone H4 ($IC_{50} = 0.005 \mu$ M), with a 40-fold higher potency with respect to that on acetylation of tubulin ($IC_{50} = 0.20 \mu$ M). It is noteworthy that 117 was very effective at inhibiting histone deacetylation at concentrations lower than those resulting as cytotoxic on the same cell lines. On the contrary, both 69 and 116 revealed similar inhibitory potency with respect to acetylation of tubulin and histone H4, with IC_{50} values resembling those measured in the cytotoxic assay on the same cells. These in vitro tests highlighted compound 117 as the best one in terms of HDAC inhibition efficacy and cytotoxic activity. It was logically selected as the drug candidate for the development of a novel oral HDAC inhibitor, and its preliminary pharmacokinetic characterization is here reported. Metabolic stability in human hepatocytes and permeability in Caco-2 cells were evaluated for prodrug 117 and for its thiol analogue 128 (Table 5). The acetyl prodrug 117 showed limited stability in human hepatocytes ($t_{1/2} \sim 2.5$ min), likely due to its hydrolysis, while the free thiol 128 was significantly more stable, with a half-life comparable to that of the reference compound 1 (~ 45 min). Permeability experiments on Caco-2 cells suggest the contribution of an active transport process to the net flux of both compounds, and the presence of digoxin reduced cellular uptake of compounds 117 and 128 by 40% and 30%, respectively. The selectivity profile of 117 and 128 was evaluated on a panel of 40 different receptors, ion channels, and enzymes. Both compounds did not significantly interact with any of the targets at the concentration of 10^{-5} M, with the only exception of compound 128, causing 45% displacement of radiolabeled reference compound at the CCK1 receptor. Such results suggest a substantial safety of compound 117, while the corresponding drug 128 could have a low probability of gastrointestinal disturbance due to the modest affinity versus theolecystokinin receptor CCK1 (Supporting Information Table S6). Plasma stability for prodrug 117 was also measured, having $t_{1/2} = 26$ min, with $10 \pm 1.6\%$ compound left after 2 h.

A systematic exploration was performed with the aim to identify a suitable vehicle to both oral and parenteral administration of compound 117. A series of surfactants and cosolvents miscible or soluble in water were investigated. The cosolvents and surfactants evaluated in this study are all excipients normally used in the development of a formulation.³⁵ Compound 117 was soluble (>10 mg/mL) in a few of excipients tested (Supporting Information Table S7). These organic solutions were then diluted in water (1/20) in order to verify their stability under these conditions. The ability or inability to form micellar systems or microemulsions was also taken as an additional selection criterion. The vehicle chosen was the Solutol HS15, diluted in water (1/20). This solution did not interfere with membrane glycoproteins nor did it influence the oral bioavailability of the compound. Furthermore, the same vehicle is suitable for a parenteral formulation.

The efficacy of compound 117 was tested in vivo, assessing its antitumor activity in two human solid tumors: a colon carcinoma HCT116 and an ovarian A2780 tumor xenograft models. The compound was administered by the oral route once daily according to the schedules qdx5/wx3w or qdx5/wx2w. Against HCT116 colon cancer, compound 117 at the dose of 60 mg/kg showed to significantly inhibit the tumor volume (TVI = 62%, $P < 0.05$) without any sign of toxicity (Table 6 and Figure 6). The free drug 128 was less active (TVI = 27%), supporting the importance of the prodrug derivatiza-

Table 5. Metabolic Stability of Selected HDAC Inhibitors in Human Hepatocytes and Permeability in Caco-2 Cells with and without Digoxin^a

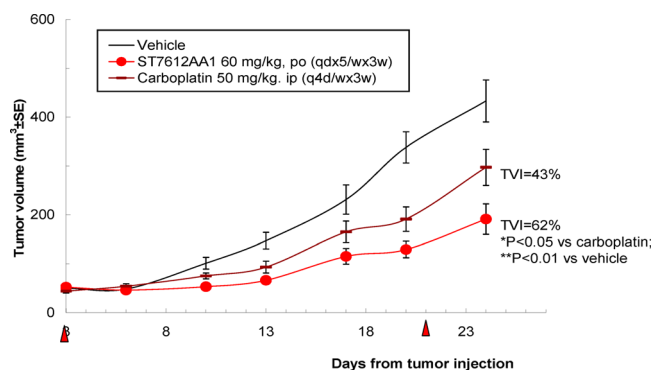
compd	ST code number	$T_{1/2}$ (min)	Cl_{int} ($\mu\text{L}/\text{min}/1 \times 10^6$ cells) ^b	Cl_{int} (mL/min/kg) ^c	AB/BA efflux ratio ^d	AB/BA efflux ratio with digoxin coincubated ^e
1		47.5	14.7	35.3		1.1
117	ST7612	2.7	252.3	605.6	6.9	4.2
128	ST7464	45.0	15.4	37.0	5.2	3.6

^aValues are the means of a minimum of three experiments. ^b Cl_{int} values are calculated considering 1×10^6 cells/mL. ^c Cl_{int} values are calculated considering 120×10^6 cells/g liver and 20 g liver/kg body weight. ^dRatio of flux in the apical:basolateral (AB) direction to flux in the basolateral:apical (BA) direction. ^eEfflux ratio (AB/BA) values with digoxin coincubated with test and reference compounds.

Table 6. Antitumor Activity of Compounds 117 and 128, delivered by the Oral Route According to the Schedule (qdx5/wx3w), against HCT116 Colon Carcinoma Cells, In Comparison to Carboplatin, and of Compound 117 in A2780 Ovarian Carcinoma Cells, in Comparison to Compound 1 (SAHA, Vorinostat), Xenografted in CD1 Nude Mice

	compd	ST code number	dose (mg/kg)	TVI ^a (%)	BWL ^b (%)
HCT116 colon cancer	117	ST7612	60	62	1
	128	ST7464	100	27	3
	carboplatin ^c		50	43	
A2780 ovarian cancer	117	ST7612	60	89	7
	1		100	53	4

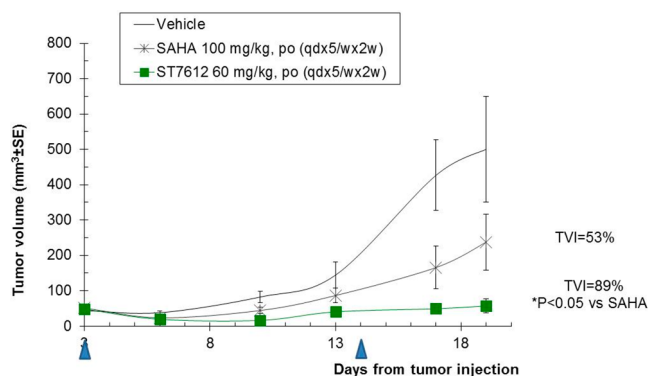
^aTumor volume inhibition. ^bBody weight loss. ^cCarboplatin was administered according to the schedule q4d/wx3w.

**Figure 6.** Antitumor activity of compound 117 (ST7612AA1) and carboplatin against HCT116 colon carcinoma xenografted in CD1 nude mice. TVI = tumor volume inhibition. Schedule qdx5/wx3w, where red triangles indicate first and last day of treatments.

tion to achieve an improved distribution. Carboplatin, used as reference compound, administered at the dose of 50 mg/kg intraperitoneally (q4d/wx3w), was characterized by a lower efficacy, having a TVI of 43%. On A2780 ovarian cancer, compound 117 revealed a potent and significant antitumor effect (TVI = 89%, $P < 0.05$) when administered at the dose of 60 mg/kg, higher than that found with the reference compound 1 (TVI = 53%) at the dose of 100 mg/kg (Figure 7).

CONCLUSIONS

Extensive research on HDAC's structure and function has led to a progressively deeper knowledge of their role in pathophysiological conditions and has revealed wider areas for therapeutic applications of HDAC inhibitors. The recent

**Figure 7.** Antitumor activity of compound 117 (ST7612AA1) and 1 (SAHA, vorinostat) against A2780 ovarian carcinoma xenografted in CD1 nude mice. TVI = tumor volume inhibition. Schedule qdx5/wx2w where blue triangles indicate first and last day of treatments.

findings of overexpression of certain HDAC isoforms, differing in each tumor, might suggest a greater therapeutic efficacy for selective HDAC inhibitors or mainly selective toward a single class, even if so far the most successful HDAC inhibitors are pan-inhibitors. From a medicinal chemistry point of view, the challenge is to identify new small molecules as new effective inhibitors, and a lot of attention has been focused on specific changes of the classic pharmacophore model.

We reported a systematic study aimed at evaluating a new class of pan-HDAC inhibitors, having a thiol as ZBG and a lactam carboxamide substituent in ω position of the polymethylene chain, and their prodrugs as in vivo agents. This combination significantly increased HDAC inhibition as well as the antiproliferative activity on various cancer cell lines when compared to unsubstituted counterparts. The inhibitory activities shown were compared with those from both their linear analogues and their hydroxamic acid analogues counterparts. It was observed that the in vitro activity did not change much going through β -, γ -, and δ -lactam, whereas stereochemistry in the ω position was very significant, being the *S*-configuration of the lactam carboxamide greatly favored over the *R*-configuration. A selection of the best protective group for the thiol ZBG was also made. The acetyl-derivatives were stable when evaluated under different pH conditions, being active in cytotoxicity studies on cancer cell lines. A graphical summary of the most relevant SARs observed for this class of compounds is depicted in Figure 8.

After a primary extensive screening in vitro, followed by the assessment of efficacy for selected compounds through in vivo studies, we selected a potential drug candidate, ST7612AA1 (117), and its preclinical assessment is currently in a phase of completion. This thioderivative may represent a progenitor of a new class of synthetic compounds that, through the

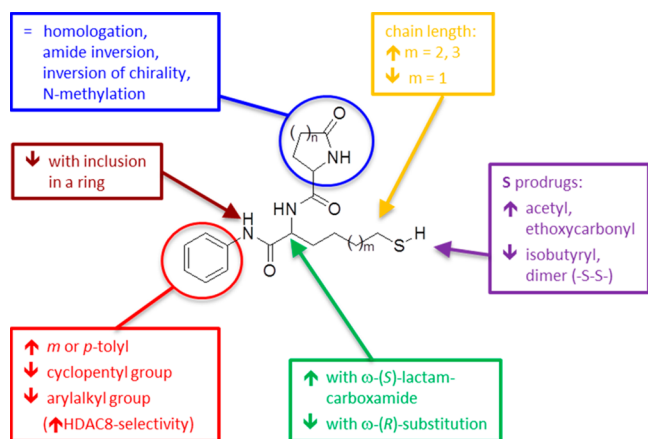


Figure 8. Graphical representation of structure–activity relationships for thiol HDAC inhibitors.

replacement of the phenyl ring with bulkier residues on CAP, could lead to more selective derivatives toward a single class or a single isoform, in an area of great therapeutic importance as well as of pharmaceutical interest.

Development of new generation HDAC inhibitors (isoform-selective or pan-inhibitors) remains an important medical need for single-agent and/or combination chemotherapy. Their association with other epigenetic target modulators could be also exploited according to what recent therapeutic approaches are suggesting.¹² The drug candidate **117** could represent a novel therapeutic agent useful in all those diseases where an epigenetic modulation is required. Compound **117** is actually under preclinical investigation studies to become a candidate to phase I clinical trials.

EXPERIMENTAL SECTION

General Procedures. Reagents were purchased from commercial suppliers and used without further purification. All nonaqueous reactions were run in flame-dried glassware under a positive pressure of argon. The exclusion of moisture from reagents and glassware was performed following standard techniques for manipulating air-sensitive compounds. Anhydrous THF, toluene, Et₂O, and DCM were obtained by filtration through drying columns (Solvent Delivery System); other solvents were distilled under positive pressure of dry argon before use and dried by standard methods. Flash chromatography was performed on 230–400 mesh silica gel with the indicated solvent systems. Thin layer chromatographies (TLCs) were performed on precoated, glass-backed silica gel plates (Merck 60F254). Visualization was performed under short-wavelength ultraviolet light and/or by dipping the plates in an aqueous H₂SO₄ solution of cerium sulfate/ammonium molybdate, potassium permanganate, or ethanolic solution of anisaldehyde, followed by charring with a heat gun. Alternatively, TLC can be stained by exposing them to iodine vapor into a iodine development chamber. Nuclear magnetic resonance spectra were recorded on Gemini spectrometers (Varian) at 300 or 500 MHz or on Bruker spectrometer at 300 MHz. Peak positions are given in parts per million downfield from tetramethylsilane as the internal standard; *J* values are expressed in hertz. Mass analyses were performed on Waters ZQ2000 spectrometer using electrospray (ES) technique. LCMS analyses were performed on a LC-Waters apparatus (HPLC Waters Alliance 2695, ZQ2000 MS, and PDA-UV detector 2996) equipped with a Phenomenex Gemini C6-Phenyl (3 μm, 150 mm × 4.6 mm), and all compounds tested were determined to be >98% pure using this method.

HRMS for **117** and **128** were performed on a Thermo Scientific Orbitrap Exactive equipped with an ESI source.

***N*-Phenylhept-6-enamide (3).** A solution of hept-6-enoic acid (1.88 g, 14.7 mmol), DIPEA (7.68 mL, 44 mmol), and aniline (1.47 mL, 16.2 mmol) was stirred at RT in DCM (100 mL) for 20 min before adding PyBOP (7.65 g, 14.7 mmol) and anhydrous DMF (10 mL). The reaction mixture was stirred for 2 h at RT. The solvent was removed under reduced pressure, and the crude reaction mixture was diluted with AcOEt, washed with 5% Na₂CO₃, water, and then with 5% aqueous citric acid, and finally with brine. After removal of the solvent under reduced pressure and purification on silica gel (*n*-hexane/AcOEt: 9/1), the desired adduct **3** was obtained (85%). ¹H NMR (300 MHz, DMSO-*d*₆) δ: 1.32–1.43 (m, 2H), 1.53–1.63 (m, 2H), 2.03 (q, *J* = 6.9 Hz, 2H), 2.29 (t, *J* = 7.4 Hz, 2H), 4.91–5.03 (m, 2H), 5.73–5.86 (m, 1H), 7.00 (t, *J* = 7.3 Hz, 1H), 7.26 (t, *J* = 7.8 Hz, 2H), 7.57 (d, *J* = 8.3 Hz, 2H), 9.84 (s, 1H). ESI-MS *m/z* 204.1 (M + H)⁺.

Compounds **4–8** were prepared similarly from hept-6-enoic acid and the corresponding amines.

(*S*)-(7-Anilino-7-oxo-heptyl) ethanethioate (9). To a stirred solution of *N*-phenylhept-6-enamide **3** (250 mg, 0.78 mmol) and thioacetic acid (564 μL, 7.8 mmol) at 75 °C in degassed dioxane was added AIBN (129 mg, 0.78 mmol). The reaction mixture was stirred for 1 h. The reaction mixture was cooled to 0 °C, and an excess of cyclohexene was added under stirring, the latter being maintained for 20 min. The reaction mixture was concentrated under reduced pressure, and the resulting crude product was rinsed more times with hexane to afford the desired adduct **9** (81%). ¹H NMR (300 MHz, DMSO-*d*₆) δ: 1.40–1.20 (m, 4H), 1.44–1.60 (m, 4H), 2.26 (t, *J* = 7.3 Hz, 2H), 2.29 (s, 3H), 2.80 (t, *J* = 7.2 Hz, 2H), 6.99 (t, *J* = 7.4 Hz, 1H), 7.25 (t, *J* = 8.2 Hz, 2H), 7.57 (d, *J* = 7.6 Hz, 2H), 9.81 (s, 1H). ESI-MS *m/z* 280.3 (M + H)⁺.

Compounds **10–14** were prepared similarly from **5–8**.

Thioacetic Acid 5-[7-(3,4-Dihydro-1*H*-isoquinolin-2-yl)-7-oxo-heptyl] Ester (10). ¹H NMR (300 MHz, DMSO-*d*₆) δ: 1.20–1.34 (m, 4H), 1.35–1.55 (m, 4H), 2.29 (s, 3H), 2.36 (t, *J* = 6.4 Hz, 2H), 2.65–2.85 (m, 4H), 3.64 (t, *J* = 6.0 Hz, 2H), 4.59 (d, *J* = 15.5 Hz, 2H), 7.16 (m, 4H). ESI-MS *m/z* 320.1 (M + H)⁺.

Thioacetic Acid 5-[6-(3-Benzoyloxy-benzylcarbamoyl)-hexyl] Ester (11). ¹H NMR (300 MHz, DMSO-*d*₆) δ: 1.20–1.28 (m, 4H), 1.43–1.57 (m, 4H), 2.11 (t, *J* = 7.3 Hz, 2H), 2.29 (s, 3H), 2.79 (t, *J* = 7.1 Hz, 2H), 4.21 (d, *J* = 5.9 Hz, 2H), 5.06 (s, 2H), 6.78–6.87 (m, 3H), 7.21 (t, *J* = 7.5 Hz, 1H), 7.31–7.43 (m, 5H), 8.26 (t, *J* = 5.6 Hz, 1H). ESI-MS *m/z* 422.3 (M + Na)⁺.

Thioacetic Acid 5-[6-(4-Trifluoromethyl-benzylcarbamoyl)-hexyl] Ester (12). ¹H NMR (300 MHz, DMSO-*d*₆) δ: 1.34–1.21 (m, 4H), 1.55–1.42 (m, 4H), 2.13 (t, *J* = 7.3 Hz, 2H), 2.30 (s, 3H), 2.80 (t, *J* = 7.2 Hz, 2H), 4.32 (d, *J* = 5.9 Hz, 2H), 7.44 (d, *J* = 7.9 Hz, 2H), 7.66 (d, *J* = 8.3 Hz, 2H), 8.37 (t, *J* = 6.0 Hz, 1H). ESI-MS *m/z* 362.3 (M + H)⁺.

5-[7-(Cyclopentylamino)-7-oxoheptyl] Ethanethioate (13). ¹H NMR (300 MHz, DMSO-*d*₆) δ: 1.16–1.37 (m, 6H), 1.38–1.52 (m, 6H), 1.54–1.65 (m, 2H), 1.68–1.80 (m, 2H), 1.99 (t, *J* = 7.5 Hz, 2H), 2.30 (s, 3H), 2.36 (t, 2H), 2.80 (t, *J* = 7.2 Hz, 2H), 3.88–4.01 (m, 1H), 7.67 (d, *J* = 6.9 Hz, 1H). ESI-MS *m/z* 272.26 (M + Na)⁺.

Thioacetic Acid 5-[6-(2-*m*-Tolyl-ethylcarbamoyl)-hexyl] Ester (14). ¹H NMR (300 MHz, DMSO-*d*₆) δ: 1.10–1.34 (m, 4H), 1.37–1.52 (m, 4H), 2.00 (t, *J* = 7.4 Hz, 2H), 2.26 (s, 3H), 2.30 (s, 3H), 2.63 (t, *J* = 7.0 Hz, 2H), 2.80 (t, *J* = 7.3 Hz, 2H), 3.17–3.27 (m, 2H), 6.93–7.02 (m, 3H), 7.11 (t, *J* = 7.7 Hz, 1H), 7.80 (t, *J* = 5.2 Hz, 1H). ESI-MS *m/z* 344.13 (M + Na)⁺.

***N*-Phenyl-7-sulfanyl-heptanamide (15).** To a stirred solution of (*S*)-(7-anilino-7-oxo-heptyl) ethanethioate **9** (322 mg, 1 mmol) in methanol (10 mL) under nitrogen at 23 °C was added sodium thiomethoxide (70 mg, 1 equiv 1 M solution in MeOH). The reaction mixture was stirred at 23 °C for 30 min. The solution was then added to aqueous HCl (20 mL/0.1M). The aqueous solution was extracted with CH₂Cl₂. The combined organic layers were washed with brine, dried over MgSO₄, filtered, and concentrated to obtain the compound **15**, which was purified through HPLC (27%). ¹H NMR (300 MHz, DMSO-*d*₆) δ: 1.32 (m, 4H), 1.54 (m, 4H), 2.20 (t, *J* = 7.4 Hz, 1H), 2.27 (t, *J* = 7.5 Hz, 2H), 2.45 (m, 2H), 6.99 (t, *J* = 7.4 Hz, 1H), 7.26 (t,

$J = 7.6$ Hz, 2H), 7.57 (d, $J = 8.5$ Hz, 2H), 9.82 (s, 1H). ESI-MS m/z 260.15 (M + Na)⁺.

Compounds **16–20** were prepared similarly from **10–14**.

1-(3,4-Dihydro-1H-isoquinolin-2-yl)-7-mercapto-heptan-1-one (16). ¹H NMR (300 MHz, DMSO-*d*₆) δ : 1.20–1.41 (m, 4H), 1.43–1.63 (m, 4H), 2.31–2.42 (m, 2H), 2.44–2.50 (m, 1H), 2.72 (t, $J = 6.1$ Hz, 1H), 2.82 (t, $J = 6.1$ Hz, 2H), 3.64 (t, $J = 6.1$ Hz, 2H), 4.59 (d, $J = 15.5$ Hz, 2H), 7.16 (bs, 4H). ESI-MS m/z 278.25 (M + H)⁺.

7-Mercapto-heptanoic Acid 3-Benzyloxy-benzylamide (17). ¹H NMR (300 MHz, DMSO-*d*₆) δ : 1.20–1.40 (m, 4H), 1.44–1.54 (m, 4H), 2.11 (t, $J = 7.4$ Hz, 2H), 2.19 (t, $J = 7.5$ Hz, 1H), 2.37–2.48 (m, 2H), 4.21 (d, $J = 5.9$ Hz, 2H), 5.06 (s, 2H), 6.76–6.90 (m, 3H), 7.16–7.26 (m, 1H), 7.28–7.46 (m, 5H), 8.26 (bt, $J = 5.8$ Hz, 1H). ESI-MS m/z 358.22 (M + H)⁺.

7-Mercapto-heptanoic Acid 4-Trifluoromethyl-benzylamide (18). ¹H NMR (500 MHz, DMSO-*d*₆) δ : 1.20–1.30 (m, 2H), 1.30–1.38 (m, 2H), 1.47–1.57 (m, 4H), 2.15 (t, $J = 7.6$ Hz, 2H), 2.20 (bs, 1H), 2.42–2.48 (m, 2H), 4.32 (d, $J = 5.8$ Hz, 2H), 7.45 (d, $J = 7.9$ Hz, 2H), 7.68 (d, $J = 7.9$ Hz, 2H), 8.39 (t, $J = 5.5$ Hz, 1H). ESI-MS m/z 319.9 (M + H)⁺.

N-Cyclopentyl-7-sulfanyl-heptanamide (19). ¹H NMR (300 MHz, DMSO-*d*₆) δ : 1.12–1.38 (m, 6H), 1.39–1.67 (m, 8H), 1.67–1.83 (m, 2H), 2.00 (t, $J = 7.2$ Hz, 2H), 2.21 (t, $J = 7.6$ Hz, 1H), 2.38–2.50 (m, 2H), 3.83–4.02 (m, 1H), 7.67 (d, $J = 6.7$ Hz, 1H). ESI-MS m/z 230.3 (M + H)⁺.

7-Mercapto-heptanoic Acid (2-m-Tolyl-ethyl)-amide (20). ¹H NMR (300 MHz, DMSO-*d*₆) δ : 1.12–1.37 (m, 4H), 1.38–1.61 (m, 4H), 2.01 (t, $J = 7.4$ Hz, 2H), 2.20 (t, $J = 6.9$ Hz, 1H), 2.26 (s, 3H), 2.38–2.47 (m, 2H), 2.63 (t, $J = 7.1$ Hz, 2H), 3.17–27 (m, 2H), 6.93–7.01 (m, 3H), 7.11–7.19 (m, 1H), 7.81 (bt, $J = 5.4$ Hz, 1H). ESI-MS m/z 280.31 (M + H)⁺.

Ethyl (7-Anilino-7-oxo-heptyl)sulfanylformate (21). To a solution of *N*-phenyl-7-sulfanyl-heptanamide **15** (50 mg, 0.21 mmol) in DCM (20 mL) were added NEt₃ (32 μ L, 0.23 mmol) and ethylchloroformate (21 mg, 0.23 mmol). The reaction mixture was stirred at RT for 2 h. The reaction mixture was concentrated under reduced pressure, and the crude product was purified through chromatography on silica gel using AcOEt/MeOH 80/20 as eluent to obtain the compound **21** (74%). ¹H NMR (300 MHz, acetone-*d*₆) δ : 1.25 (t, $J = 7.0$ Hz, 3H), 1.38–1.43 (m, 4H), 1.61–1.71 (m, 4H), 2.36 (t, $J = 7.3$ Hz, 2H), 2.86 (t, $J = 7.3$ Hz, 2H), 4.24 (q, $J = 7.0$ Hz, 2H), 7.02 (t, $J = 7.3$ Hz, 1H), 7.27 (t, $J = 7.9$ Hz, 2H), 7.65 (d, $J = 7.6$ Hz, 2H), 9.04 (s, 1H). ESI-MS m/z 332.1 (M + Na)⁺.

Compounds **22–23** were prepared similarly from **15** and isobutyryl chloride and (2*R*)-2-amino-3-methyl-butanoyl chloride, respectively.

For disulfide **24**, oxidation side product of thioacetate **9** hydrolysis, see below.

Thioisobutyric Acid S-(6-Phenylcarbamoyl-hexyl) Ester (22). ¹H NMR (300 MHz, acetone-*d*₆) δ : 1.14 (d, $J = 7.0$ Hz, 6H), 1.36–1.45 (m, 4H), 1.53–1.60 (m, 2H), 1.64–1.72 (m, 2H), 2.35 (t, $J = 7.3$ Hz, 2H), 2.68–2.78 (m, 1H), 2.85 (t, $J = 7.3$ Hz, 2H), 7.02 (t, $J = 7.6$ Hz, 1H), 7.26 (t, $J = 7.6$ Hz, 2H), 7.65 (d, $J = 8.2$ Hz, 2H), 9.03 (s, 1H). ESI-MS m/z 308.19 (M + H)⁺.

(R)-2-Amino-3-methyl-thiobutyric Acid S-(6-Phenylcarbamoyl-hexyl) Ester (23). ¹H NMR (300 MHz, DMSO-*d*₆) δ : 0.77 (d, $J = 6.8$ Hz, 3H), 0.88 (d, $J = 6.8$ Hz, 3H), 1.20–1.40 (m, 4H), 1.41–1.62 (m, 4H), 1.91–2.01 (m, 3H), 2.27 (t, $J = 7.5$ Hz, 2H), 2.75 (t, $J = 7.2$ Hz, 2H), 3.18 (d, $J = 4.8$ Hz, 1H), 7.00 (t, $J = 7.4$ Hz, 1H), 7.26 (t, $J = 8.4$ Hz, 2H), 7.56 (d, $J = 7.6$ Hz, 2H), 9.83 (s, 1H). ESI-MS m/z 337.28 (M + H)⁺.

6-(5-Phenylcarbamoyl-pentyl)disulfanyl-hexanoic Acid Phenylamide (24). A 2*N* solution of NaOH (343 mg, 7.0 mmol) was added to a solution of (S)-(7-anilino-7-oxo-heptyl) ethanethioate **9** (265 mg, 0.95 mmol) in EtOH (13 mL). The reaction mixture was stirred at RT overnight and then poured into water and extracted with AcOEt, washed with water, brine, and finally dried over Na₂SO₄. Removal of the solvent under reduced pressure led to the desired adduct as a side product **24** (20%), which was purified through HPLC. ¹H NMR (500 MHz, DMSO-*d*₆) δ : 1.34–1.42 (m, 4H), 1.56–1.68 (m, 8H), 2.29 (t, $J = 7.0$ Hz, 4H), 2.70 (t, $J = 7.0$ Hz, 4H), 7.01 (t, $J =$

7.5 Hz, 2H), 7.27 (t, $J = 8.0$ Hz, 4H), 7.58 (d, $J = 7.5$ Hz, 4H), 9.84 (s, 2H). ESI-MS m/z 445.25 (M + H)⁺.

Thiols **45–48** were isolated by HPLC, from hydrolysis mixture of their corresponding stereoisomers **37–40**, and characterized (see below). As thioacetates, only **38–39** were easily isolated.

Thioacetic Acid S-((S)-6-(((3*R*,4*S*)-2-Oxo-4-phenyl-pyrrolidine-3-carbonyl)-amino)-6-phenylcarbamoyl-hexyl) Ester (38). ¹H NMR (300 MHz, acetone-*d*₆) δ : 1.30–1.80 (m, 8H), 2.28 (s, 3H), 2.81 (t, $J = 7.5$ Hz, 2H), 3.51 (t, $J = 9.6$ Hz, 1H), 3.75 (d, $J = 10.7$ Hz, 1H), 3.82–3.92 (m, 1H), 4.25–4.37 (m, 1H), 4.47–4.60 (m, 1H), 7.00–7.40 (m, 8H), 7.53 (bs, 1H), 7.81–7.88 (m, 2H), 7.89 (d, $J = 6.6$ Hz, 1H), 9.80 (bs, 1H). ESI-MS m/z 482.1 (M + H)⁺.

Thioacetic Acid S-((S)-6-(((3*S*,4*S*)-2-Oxo-4-phenyl-pyrrolidine-3-carbonyl)-amino)-6-phenylcarbamoyl-hexyl) Ester (39). ¹H NMR (300 MHz, acetone-*d*₆) δ : 1.35–2.00 (m, 8H), 2.28 (s, 3H), 2.84 (t, $J = 7.5$ Hz, 2H), 3.40 (t, $J = 9.6$ Hz, 1H), 3.59 (d, $J = 10.7$ Hz, 1H), 3.75–3.82 (m, 1H), 4.08–4.19 (m, 1H), 4.42–4.52 (m, 1H), 7.00–7.40 (m, 9H), 7.58–7.67 (m, 2H), 7.89 (d, $J = 6.6$ Hz, 1H), 9.25 (bs, 1H). ESI-MS m/z 482.1 (M + H)⁺.

Thioacetic Acid S-((S)-6-((R/*S*)-(2-Oxo-piperidine-3-carbonyl)-amino)-6-phenyl carbamoyl-hexyl) Ester (41–42). ¹H NMR (500 MHz, CD₃OD) δ : 1.42–1.99 (m, 10H), 2.29 (s, 3H), 2.55 (t, $J = 7.2$ Hz, 2H), 2.80 (t, $J = 7.6$ Hz, 2H), 3.35 (m, 2H), 3.40 (m, 2H), 4.53 (m, 2H), 7.12 (t, $J = 7.0$ Hz, 1H), 7.33 (t, $J = 7.5$ Hz, 2H), 7.60 (d, $J = 8.5$ Hz, 2H). ESI-MS m/z 442.1 (M + Na)⁺.

(3*S*,4*R*)-2-Oxo-4-phenyl-pyrrolidine-3-carboxylic Acid ((S)-6-Mercapto-1-phenylcarbamoyl-hexyl)-amide (45). ¹H NMR (500 MHz, CD₃OD) δ : 1.24–1.50 (m, 4H), 1.50–1.61 (m, 2H), 1.64–1.74 (m, 1H), 1.95–2.05 (m, 1H), 2.42 (t, $J = 7.3$ Hz, 2H), 3.51 (t, $J = 9.6$ Hz, 1H), 3.72–3.85 (m, 3H), 4.49–4.55 (m, 1H), 7.10–7.16 (m, 1H), 7.26–7.40 (m, 7H), 7.64–7.69 (m, 2H). ESI-MS m/z 462.3 (M + Na)⁺.

(3*R*,4*S*)-2-Oxo-4-phenyl-pyrrolidine-3-carboxylic Acid ((S)-6-Mercapto-1-phenylcarbamoyl-hexyl)-amide (46). ¹H NMR (500 MHz, CD₃OD) δ : 1.25–1.50 (m, 4H), 1.50–1.60 (m, 2H), 1.65–1.75 (m, 1H), 1.95–2.05 (m, 1H), 2.44 (t, $J = 7.3$ Hz, 2H), 3.49 (t, $J = 9.6$ Hz, 1H), 3.72–3.85 (m, 2H), 4.16–4.25 (m, 1H), 4.49–4.55 (m, 1H), 7.07–7.14 (m, 1H), 7.26–7.40 (m, 7H), 7.64–7.69 (d, $J = 7.9$ Hz, 2H). ESI-MS m/z 462.3 (M + Na)⁺.

(3*S*,4*S*)-2-Oxo-4-phenyl-pyrrolidine-3-carboxylic Acid ((S)-6-Mercapto-1-phenylcarbamoyl-hexyl)-amide (47). ¹H NMR (500 MHz, CD₃OD) δ : 1.25–1.50 (m, 4H), 1.50–1.70 (m, 3H), 1.95–2.05 (m, 1H), 2.40 (t, $J = 7.3$ Hz, 2H), 3.45 (t, $J = 9.6$ Hz, 1H), 3.71–3.84 (m, 3H), 4.49–5.5 (m, 1H), 7.10–7.20 (m, 1H), 7.24–7.37 (m, 7H), 7.65–7.70 (m, 2H). ESI-MS m/z 462.3 (M + Na)⁺.

(3*R*,4*R*)-2-Oxo-4-phenyl-pyrrolidine-3-carboxylic Acid ((S)-6-Mercapto-1-phenylcarbamoyl-hexyl)-amide (48). ¹H NMR (500 MHz, CD₃OD) δ : 1.24–1.49 (m, 4H), 1.50–1.61 (m, 2H), 1.65–1.75 (m, 1H), 1.90–2.00 (m, 1H), 2.46 (t, $J = 7.3$ Hz, 2H), 3.47 (t, $J = 9.6$ Hz, 1H), 3.72–3.84 (m, 2H), 4.16–4.25 (m, 1H), 4.49–5.5 (m, 1H), 7.07–7.14 (m, 1H), 7.26–7.40 (m, 7H), 7.63–7.70 (m, 2H). ESI-MS m/z 462.3 (M + Na)⁺.

(3*R*)-2-Oxo-pyrrolidine-3-carboxylic Acid ((S)-6-Mercapto-1-phenylcarbamoyl-hexyl)-amide (49). ¹H NMR (500 MHz, CD₃OD) δ : 1.40–1.60 (m, 4H), 1.66–1.85 (m, 4H), 1.85–2.08 (m, 1H), 2.27–2.48 (m, 2H), 2.52–2.62 (m, 1H), 2.70 (m, 2H), 3.31–3.49 (m, 4H), 3.54 (t, $J = 9.2$ Hz, 1H), 4.45–4.55 (m, 1H), 7.07–7.13 (m, 1H), 7.27–7.34 (m, 2H), 7.56 (m, $J = 7.9$ Hz, 1H), 7.65 (d, $J = 7.6$ Hz, 1H). ESI-MS m/z 364.2 (M + H)⁺.

(S)-2-Oxo-piperidine-3-carboxylic Acid ((S)-6-Mercapto-1-phenylcarbamoyl-hexyl)-amide (50). ¹H NMR (500 MHz, CD₃OD) δ : 1.40–1.55 (m, 4H), 1.56–1.69 (m, 2H), 1.70–1.85 (m, 2H), 1.95–2.10 (m, 3H), 2.10–2.21 (m, 1H), 2.55 (t, $J = 7.0$ Hz, 2H), 3.41–3.46 (m, 1H), 4.44–4.49 (m, 1H), 7.09 (t, $J = 7.6$ Hz, 1H), 7.29 (t, $J = 8.2$ Hz, 2H), 7.68 (d, $J = 7.9$ Hz, 2H). ESI-MS m/z 400.4 (M + Na)⁺.

(R)-2-Oxo-piperidine-3-carboxylic Acid ((S)-6-Mercapto-1-phenylcarbamoyl-hexyl)-amide (51). ¹H NMR (500 MHz, CD₃OD) δ : 1.40–1.60 (m, 4H), 1.60–1.70 (m, 2H), 1.72–1.85 (m, 2H), 1.76–2.00 (m, 2H), 2.04–2.20 (m, 2H), 2.55 (t, $J = 7.0$ Hz, 2H), 3.40 (t, $J = 7.0$ Hz, 1H), 4.44–4.79 (m, 1H), 7.12 (t, $J = 7.3$ Hz, 1H), 7.33 (t, $J = 8.2$ Hz, 2H), 7.60 (d, $J = 7.9$ Hz, 2H). ESI-MS m/z 400.4 (M + Na)⁺.

((S)-1-Cyclopentylcarbamoyl-6-mercapto-hexyl)-carbamic acid *tert*-butyl ester (**52**) and thioisobutyric acid *S*-((S)-6-*tert*-butoxycarbonylamino-6-cyclopentylcarbamoyl-hexyl) ester (**53**) were synthesized following the synthetic method described in the literature.²⁰

((S)-1-Phenylcarbamoyl-hex-5-enyl)-carbamic Acid *tert*-Butyl Ester (**54**). A solution of (S)-2-*tert*-butoxycarbonylamino-hept-6-enoic acid (745 mg, 5.24 mmol), DIPEA (2.74 mL, 15.7 mmol), and aniline (525 μ L, 5.76 mmol) was stirred at RT in DCM (70 mL) for 20 min before adding PyBOP (2.73 g, 5.24 mmol) and anhydrous DMF (5 mL). The reaction mixture was stirred for 2 h at RT. The solvent was removed under reduced pressure, and the crude reaction mixture was diluted with AcOEt, washed with 5% Na₂CO₃, water, and then with 5% aqueous citric acid and finally with brine. After removal of the solvent under reduced pressure and purification on silica gel (*n*-hexane/AcOEt: 9/1), the desired adduct **54** was obtained (85%). ¹H NMR (300 MHz, DMSO-*d*₆) δ : 1.20–1.72 (m, 13H), 1.93–2.10 (m, 2H), 3.98–4.12 (m, 1H), 4.88–5.05 (m, 2H), 5.70–5.85 (m, 1H), 7.02 (t, *J* = 7.4 Hz, 2H), 7.29 (t, *J* = 7.5 Hz, 2H), 7.59 (d, *J* = 8.6 Hz, 2H), 9.92 (s, 1H). ESI-MS *m/z* 341.2 (M + Na)⁺.

Compounds **55**–**58** were prepared similarly from the corresponding amines.

Thioacetic Acid S-((S)-6-*tert*-Butoxycarbonylamino-6-phenylcarbamoyl-hexyl) Ester (**59**). To a stirred solution of ((S)-1-phenylcarbamoyl-hex-5-enyl)-carbamic acid *tert*-butyl ester **54** (250 mg, 0.78 mmol) and thioacetic acid (564 μ L, 7.8 mmol) at 75 °C in degassed dioxane was added AIBN (129 mg, 0.78 mmol). The reaction mixture was stirred for 1 h. The reaction mixture was cooled to 0 °C, and an excess of cyclohexene was added under stirring, the latter being maintained for 20 min. The reaction mixture was concentrated under reduced pressure, and the resulting crude product was rinsed more times with hexane to afford the desired adduct **59** (81%). ¹H NMR (300 MHz, DMSO-*d*₆) δ : 1.20–1.40 (m, 13H), 1.40–1.70 (m, 4H), 2.29 (s, 3H), 2.79 (t, *J* = 7.2 Hz, 2H), 3.95–4.09 (m, 1H), 6.96 (d, *J* = 7.9 Hz, 1H), 7.02 (t, *J* = 7.3 Hz, 1H), 7.28 (t, *J* = 8.4 Hz, 2H), 7.57 (d, *J* = 8.6 Hz, 2H), 9.89 (s, 1H). ESI-MS *m/z* 417.2 (M + Na)⁺.

Compounds **60**–**63** were prepared similarly **55**–**58**.

Thioacetic Acid S-((S)-6-Amino-6-phenylcarbamoyl-hexyl) Ester (**64**). To a stirred solution in DCM (20 mL) of thioacetic acid *S*-((S)-6-*tert*-butoxycarbonylamino-6-phenylcarbamoyl-hexyl) ester **59** (103 mg, 0.35 mmol) at 0 °C was added TFA (4 mL) slowly. The reaction mixture was then allowed to warm to RT and stirred overnight. The solvent was removed under reduced pressure to afford the desired adduct **64** as the trifluoroacetate salt, which was used without any purification in the next step.

Compounds **65**–**68** were prepared similarly from **60**–**63**.

Thioacetic Acid S-((S)-6-(((S)-4-Oxo-azetidine-2-carbonyl)-amino)-6-phenylcarbamoyl-hexyl) Ester (**69**). To a solution of the trifluoroacetate salt **64** as obtained in step C (305 mg, 0.75 mmol) in DCM (10 mL) were added NEt₃ (312 μ L, 2.24 mmol), (S)-4-oxo-azetidine-2-carboxylic acid (90 mg, 0.79 mmol), PyBOP (408 mg, 0.79 mmol), and DMF (1.7 mL). The reaction mixture was stirred overnight and then diluted with AcOEt, washed with water, 5% aq Na₂CO₃, brine 5% citric acid solution, and brine again. The crude material was purified through chromatography on silica gel using AcOEt as eluent to allow the desired adduct **69** as a white solid (42%). ¹H NMR (300 MHz, DMSO-*d*₆) δ : 1.20–1.40 (m, 4H), 1.40–1.54 (m, 2H), 1.55–1.78 (m, 2H), 2.29 (s, 3H), 2.67 (dt, *J*₁ = 14.5 Hz, *J*₂ = 2.1 Hz, 1H), 2.79 (t, *J* = 7.2 Hz, 2H), 3.09 (dd, *J*₁ = 14.4 Hz, *J*₂ = 5.4 Hz, 1H), 4.06 (dd, *J*₁ = 5.4 Hz, *J*₂ = 2.4 Hz, 1H), 4.37–4.47 (m, 1H), 7.03 (t, *J* = 7.5 Hz, 1H), 7.28 (t, *J* = 8.4 Hz, 2H), 7.57 (d, *J* = 8.7 Hz, 2H), 8.12 (s, 1H), 8.38 (d, *J* = 8.1 Hz, 1H), 10.07 (s, 1H). ESIMS *m/z* 392.0 (M + H)⁺. ESI-MS *m/z* 504.2 (M + CF₃COO)⁻.

Compounds **70**–**79** were prepared similarly from trifluoroacetate salts **64**–**68** and the corresponding carboxylic acids.

Thioacetic Acid S-((S)-6-(((S)-5-Oxo-pyrrolidine-2-carbonyl)-amino)-6-phenylcarbamoyl-hexyl) Ester (**70**). ¹H NMR (300 MHz, DMSO-*d*₆) δ : 1.20–1.40 (m, 4H), 1.41–1.54 (m, 2H), 1.55–1.75 (m, 2H), 1.80–1.92 (m, 1H), 1.95–2.27 (m, 3H), 2.28 (s, 3H), 2.79 (t, *J* = 7.2 Hz, 2H), 4.05–4.11 (m, 1H), 4.32–4.42 (m, 1H), 7.02 (t, *J* = 7.3 Hz, 1H), 7.28 (t, *J* = 7.8 Hz, 2H), 7.56 (d, *J* = 8.2 Hz, 2H), 7.77 (s,

1H), 8.19 (d, *J* = 8.1 Hz, 1H), 10.03 (s, 1H). ESI-MS *m/z* 406.4 (M + H)⁺.

Thioacetic acid S-((S)-6-(((S)-1-Methyl-6-oxo-piperidine-2-carbonyl)-amino)-6-phenylcarbamoyl-hexyl) Ester (**71**). ¹H NMR (300 MHz, DMSO-*d*₆) δ : 1.20–1.41 (m, 4H), 1.42–1.78 (m, 5H), 1.79–2.01 (m, 2H), 2.17 (bt, *J* = 6.6 Hz, 2H), 2.29 (s, 3H), 2.68 (s, 3H), 2.79 (t, *J* = 7.0 Hz, 2H), 4.04–4.07 (m, 1H), 4.39–4.49 (m, 1H), 7.03 (t, *J* = 7.2 Hz, 1H), 7.29 (t, *J* = 7.3 Hz, 2H), 7.57 (d, *J* = 8.2 Hz, 2H), 8.34 (d, *J* = 7.6 Hz, 1H), 10.06 (s, 1H). ESI-MS *m/z* 433.9 (M + H)⁺.

Thioacetic Acid S-((S)-6-(((S)-6-Oxo-1,2,3,6-tetrahydro-pyridine-2-carbonyl)-amino)-6-phenylcarbamoyl-hexyl) Ester (**72**). ¹H NMR (300 MHz, DMSO-*d*₆) δ : 1.18–1.38 (m, 4H), 1.40–1.75 (m, 4H), 2.28 (s, 3H), 2.50–2.58 (m, 2H), 2.78 (t, *J* = 7.2 Hz, 2H), 4.04–4.12 (m, 1H), 4.33–4.43 (m, 1H), 5.61–5.68 (m, 1H), 6.45–6.55 (m, 1H), 7.03 (t, *J* = 7.3 Hz, 1H), 7.28 (t, *J* = 8.4 Hz, 2H), 7.43–4.9 (m, 1H), 7.56 (d, *J* = 8.7 Hz, 2H), 8.01 (d, *J* = 7.9 Hz, 1H), 10.03 (s, 1H). ESI-MS *m/z* 440.1 (M + Na)⁺.

Thioacetic Acid S-((R)-1-Methyl-5-oxo-pyrrolidine-2-carbonyl)-amino)-6-phenylcarbamoyl-hexyl) Ester (**73**). ¹H NMR (300 MHz, DMSO-*d*₆) δ : 1.20–1.41 (m, 4H), 1.42–1.56 (m, 2H), 1.57–1.75 (m, 2H), 1.76–1.92 (m, 1H), 2.07–2.29 (m, 3H), 2.31 (s, 3H), 2.61 (s, 3H), 2.82 (t, *J* = 7.1 Hz, 2H), 4.09–4.18 (m, 1H), 4.36–4.45 (m, 1H), 7.05 (t, *J* = 7.4 Hz, 1H), 7.31 (t, *J* = 8.2 Hz, 2H), 7.9 (d, *J* = 7.6 Hz, 2H), 8.50 (d, *J* = 7.8 Hz, 1H), 10.10 (s, 1H). ESI-MS *m/z* 420.2 (M + H)⁺.

Thioacetic Acid S-((S)-6-(((S)-6-Oxo-piperidine-2-carbonyl)-amino)-6-(2-*m*-tolyl-ethylcarbamoyl)-hexyl) Ester (**74**). ¹H NMR (300 MHz, DMSO-*d*₆) δ : 1.06–1.32 (m, 4H), 1.36–1.76 (m, 7H), 1.76–1.92 (m, 1H), 2.10 (t, *J* = 6.5 Hz, 2H), 2.26 (s, 3H), 2.30 (s, 3H), 2.65 (t, *J* = 7.1 Hz, 2H), 2.78 (t, *J* = 7.2 Hz, 2H), 3.12–3.30 (m, 2H), 3.85–4.95 (m, 1H), 4.10–4.22 (m, 1H), 6.93–7.03 (m, 3H), 7.14 (t, *J* = 7.9 Hz, 1H), 7.50 (d, *J* = 2.5 Hz, 1H), 7.85–8.00 (m, 2H). ESI-MS *m/z* 462.1 (M + H)⁺.

Thioacetic Acid S-((S)-7-(3,4-Dihydro-1H-isoquinolin-2-yl)-7-oxo-6-(((S)-6-oxo-piperidine-2-carbonyl)-amino)-heptyl) Ester (**75**). ¹H NMR (300 MHz, DMSO-*d*₆) δ : 1.20–1.36 (m, 4H), 1.37–1.90 (m, 9H), 2.07 (m, 2H), 2.29 (s, 3H), 2.71–2.90 (m, 3H), 3.64–3.75 (m, 2H), 3.81–3.95 (m, 1H), 4.49–4.70 (m, 2H), 4.71–4.83 (m, 1H), 7.17 (s, 4H), 7.45–7.50 (m, 1H), 8.06–8.16 (m, 1H). ESI-MS *m/z* 460.2 (M + H)⁺.

Thioacetic Acid S-((S)-6-(((S)-5-Oxo-pyrrolidine-2-carbonyl)-amino)-6-*m*-tolylcarbamoyl-hexyl) Ester (**76**). ¹H NMR (300 MHz, DMSO-*d*₆) δ : 1.20–1.43 (m, 4H), 1.44–1.76 (m, 4H), 1.83–1.96 (m, 1H), 2.00–2.226 (m, 3H), 2.27 (s, 3H), 2.31 (s, 3H), 2.81 (t, *J* = 7.2 Hz, 2H), 4.07–4.14 (m, 1H), 4.33–4.43 (m, 1H), 6.87 (d, *J* = 7.5 Hz, 1H), 7.18 (t, *J* = 7.8 Hz, 1H), 7.37 (d, *J* = 8.5 Hz, 1H), 7.42 (s, 1H), 7.79 (s, 1H), 8.19 (d, *J* = 7.8 Hz, 1H), 9.96 (s, 1H). ESI-MS *m/z* 420.3 (M + H)⁺.

Thioacetic Acid S-((S)-6-(((R)-5-Oxo-pyrrolidine-2-carbonyl)-amino)-6-*m*-tolylcarbamoyl-hexyl) Ester (**77**). ¹H NMR (300 MHz, DMSO-*d*₆) δ : 1.20–1.40 (m, 4H), 1.41–1.76 (m, 4H), 1.78–1.91 (m, 1H), 1.99–2.24 (m, 3H), 2.25 (s, 3H), 2.29 (s, 3H), 2.79 (t, *J* = 7.2 Hz, 2H), 4.05–4.13 (m, 1H), 4.34–4.45 (m, 1H), 6.85 (d, *J* = 7.5 Hz, 1H), 7.16 (t, *J* = 7.9 Hz, 1H), 7.36 (d, *J* = 7.9 Hz, 1H), 7.40 (s, 1H), 7.80 (s, 1H), 8.15 (d, *J* = 8.1 Hz, 1H), 9.96 (s, 1H). ESI-MS *m/z* 420.3 (M + H)⁺.

Thioacetic Acid S-((S)-6-(((R)-1-Methyl-5-oxo-pyrrolidine-2-carbonyl)-amino)-6-*m*-tolylcarbamoyl-hexyl) Ester (**78**). ¹H NMR (300 MHz, DMSO-*d*₆) δ : 1.20–1.40 (m, 4H), 1.41–1.87 (m, 5H), 2.03–2.24 (m, 3H), 2.25 (s, 3H), 2.28 (s, 3H), 2.58 (s, 3H), 2.80 (t, *J* = 7.2 Hz, 2H), 4.09–4.18 (m, 1H), 4.31–4.43 (m, 1H), 6.85 (d, *J* = 7.5 Hz, 1H), 7.16 (t, *J* = 7.8 Hz, 1H), 7.36 (d, *J* = 8.7 Hz, 1H), 7.40 (s, 1H), 8.47 (d, *J* = 7.6 Hz, 1H), 9.99 (s, 1H). ESI-MS *m/z* 434.4 (M + H)⁺; 546.5 (M + CF₃COO)⁻.

Thioacetic Acid S-((S)-6-(((R)-5-Oxo-pyrrolidine-2-carbonyl)-amino)-6-(3-trifluoromethyl-phenylcarbamoyl)-hexyl) Ester (**79**). ¹H NMR (300 MHz, DMSO-*d*₆) δ : 1.20–1.40 (m, 4H), 1.42–1.78 (m, 4H), 1.78–1.90 (m, 1H), 2.28 (s, 3H), 2.00–2.34 (m, 3H), 2.79 (t, *J* = 7.2 Hz, 2H), 4.05–4.13 (m, 1H), 4.32–4.42 (m, 1H), 7.39 (d, *J* = 7.8 Hz, 1H), 7.54 (t, *J* = 8.2 Hz, 1H), 7.74–7.84 (m, 2H), 8.08 (s,

1H), 8.26 (d, $J = 8.1$ Hz, 1H), 10.43 (s, 1H). ^{19}F NMR (282 MHz, $\text{DMSO-}d_6$) δ : -62.97. ESI-MS m/z 474.3 (M + H) $^+$; 586.3 (M + CF_3COO) $^-$.

(*S*)-4-Oxo-azetidine-2-carboxylic Acid ((*S*)-6-Mercapto-1-phenylcarbamoyl-hexyl)-amide (**80**). To a stirred solution of thioacetate **69** (392 mg, 1 mmol) in methanol (10 mL) under nitrogen at 23 °C was added sodium thiomethoxide (70 mg, 1 equiv 1 M solution in MeOH). The reaction mixture was stirred at 23 °C for 30 min. The solution was then added to aqueous HCl 20 mL/0.1M). The aqueous solution was extracted with CH_2Cl_2 . The combined organic layers were washed with brine, dried over MgSO_4 , filtered, and concentrated to obtain the compound **80**, which was purified through HPLC (27%). ^1H NMR (300 MHz, $\text{DMSO-}d_6$) δ : 1.20–1.41 (m, 4H), 1.43–1.80 (m, 4H), 2.22 (t, $J = 7.0$ Hz, 1H), 2.40–2.50 (m, 1H), 2.60–2.73 (m, 2H), 3.10 (dd, $J_1 = 14.3$ Hz, $J_2 = 5.3$ Hz, 1H), 4.07 (dd, $J_1 = 5.3$ Hz, $J_2 = 2.3$ Hz, 1H), 4.37–4.50 (m, 1H), 7.04 (t, $J = 7.4$ Hz, 1H), 7.29 (t, $J = 7.7$ Hz, 2H), 7.58 (d, $J = 8.2$ Hz, 2H), 8.16 (s, 1H), 8.43 (d, $J = 8.0$ Hz, 1H), 10.11 (s, 1H). ESI-MS m/z 372.2 (M + Na) $^+$; 348.2 (M – H) $^-$.

Compounds **81**–**89** were prepared similarly from **70**, **71**, and **73**–**79**.

(2*S*)-5-Oxo-*N*-[(1*S*)-1-(phenylcarbamoyl)-6-sulfanyl-hexyl]pyrrolidine-2-carboxamide (**81**). ^1H NMR (300 MHz, $\text{DMSO-}d_6$) δ : 1.20–1.45 (m, 4H), 1.47–1.80 (m, 4H), 1.81–1.97 (m, 1H), 2.01–2.25 (m, 4H), 2.41–2.50 (m, 2H), 4.07–4.15 (m, 1H), 4.35–4.47 (m, 1H), 7.05 (t, $J = 7.4$ Hz, 1H), 7.31 (t, $J = 8.3$ Hz, 2H), 7.61 (d, $J = 8.1$ Hz, 2H), 7.80 (s, 1H), 8.20 (d, $J = 7.9$ Hz, 1H), 10.05 (s, 1H). ESI-MS m/z 364.2 (M + H) $^+$.

(*S*)-1-Methyl-6-oxo-piperidine-2-carboxylic Acid ((*S*)-6-Mercapto-1-phenylcarbamoyl-hexyl)-amide (**82**). ^1H NMR (300 MHz, $\text{DMSO-}d_6$) δ : 1.20–1.45 (m, 4H), 1.46–1.80 (m, 6H), 1.80–2.03 (m, 2H), 2.15–2.25 (m, 3H), 2.40–2.50 (m, 2H), 2.69 (s, 3H), 4.03–5.02 (m, 1H), 4.40–4.50 (m, 1H), 7.05 (t, $J = 7.4$ Hz, 1H), 7.30 (t, $J = 7.6$ Hz, 2H), 7.58 (d, $J = 8.1$ Hz, 2H), 8.35 (d, $J = 7.9$ Hz, 1H), 10.08 (s, 1H). ESI-MS m/z 392.0 (M + H) $^+$.

(2*R*)-1-Methyl-5-oxo-*N*-[(1*S*)-1-(phenylcarbamoyl)-6-sulfanyl-hexyl]pyrrolidine-2-carboxamide (**83**). ^1H NMR (300 MHz, $\text{DMSO-}d_6$) δ : 1.20–1.45 (m, 4H), 1.45–1.90 (m, 5H), 2.20–2.35 (m, 4H), 2.35–2.50 (m, 2H), 2.61 (s, 3H), 4.11–4.20 (m, 1H), 4.35–4.47 (m, 1H), 7.05 (t, $J = 7.4$ Hz, 1H), 7.30 (t, $J = 7.4$ Hz, 2H), 7.59 (d, $J = 8.3$ Hz, 2H), 8.50 (d, $J = 7.7$ Hz, 1H), 10.09 (s, 1H). ESI-MS m/z 378.2 (M + H) $^+$.

(*S*)-6-Oxo-piperidine-2-carboxylic Acid [(*S*)-6-Mercapto-1-(2-*m*-tolyl-ethylcarbamoyl)-hexyl]-amide (**84**). ^1H NMR (300 MHz, $\text{DMSO-}d_6$) δ : 1.10–1.34 (m, 4H), 1.42–1.53 (m, 3H), 1.54–1.76 (m, 4H), 1.80–1.89 (m, 1H), 2.11 (t, $J = 6.4$ Hz, 2H), 2.21 (t, $J = 7.9$ Hz, 1H), 2.27 (s, 3H), 2.40–2.48 (m, 2H), 2.66 (t, $J = 7.0$ Hz, 2H), 3.16–3.26 (m, 2H), 3.90–3.95 (m, 1H), 4.15–4.25 (m, 1H), 6.95–7.05 (m, 3H), 7.16 (t, $J = 7.9$ Hz, 1H), 7.51 (d, $J = 2.1$ Hz, 1H), 7.89 (d, $J = 8.2$ Hz, 1H), 7.95 (t, $J = 5.5$ Hz, 1H). ESI-MS m/z 420.1 (M + H) $^+$.

(*S*)-6-Oxo-piperidine-2-carboxylic Acid [(*S*)-1-(3,4-Dihydro-1*H*-isoquinoline-2-carbonyl)-6-mercapto-hexyl]-amide (**85**). ^1H NMR (300 MHz, $\text{DMSO-}d_6$) δ : 1.10–1.90 (m, 13H), 2.05–2.23 (m, 2H), 2.35–3.00 (m, 4H), 3.60–4.10 (m, 3H), 4.48–4.86 (m, 3H), 7.17 (s, 4H), 7.49 (m, 1H), 8.10 (m, 4H). ESI-MS m/z 418.1 (M + H) $^+$.

(2*S*)-*N*-[(1*S*)-1-(*m*-Tolylcarbamoyl)-6-sulfanyl-hexyl]-5-oxo-pyrrolidine-2-carboxamide (**86**). ^1H NMR (300 MHz, $\text{DMSO-}d_6$) δ : 1.20–1.42 (m, 4H), 1.45–1.78 (m, 4H), 1.80–1.93 (m, 1H), 1.95–2.25 (m, 3H), 2.26 (s, 3H), 2.40–2.50 (m, 2H), 4.06–4.13 (m, 1H), 4.33–4.43 (m, 1H), 6.86 (d, $J = 7.3$ Hz, 1H), 7.17 (t, $J = 7.9$ Hz, 1H), 7.36 (d, $J = 8.1$ Hz, 1H), 7.42 (s, 1H), 7.78 (s, 1H), 8.15 (d, $J = 7.7$ Hz, 1H), 9.95 (s, 1H). ESI-MS m/z 378.2 (M + H) $^+$.

(2*R*)-*N*-[(1*S*)-1-(*m*-Tolylcarbamoyl)-6-sulfanyl-hexyl]-5-oxo-pyrrolidine-2-carboxamide (**87**). ^1H NMR (300 MHz, $\text{DMSO-}d_6$) δ : 1.20–1.41 (m, 4H), 1.42–1.72 (m, 4H), 1.75–1.97 (m, 1H), 2.00–2.40 (m, 6H), 2.38–2.50 (m, 2H), 4.06–4.14 (m, 1H), 4.34–4.46 (m, 1H), 6.86 (d, $J = 7.7$ Hz, 1H), 7.17 (t, $J = 7.8$ Hz, 1H), 7.37 (d, $J = 8.4$ Hz, 1H), 7.41 (s, 1H), 7.81 (s, 1H), 8.15 (d, $J = 7.9$ Hz, 1H), 9.96 (s, 1H). ESI-MS m/z 378.1 (M + H) $^+$; 376.1 (M – H) $^-$.

(2*R*)-1-Methyl-*N*-[(1*S*)-1-(*m*-Tolylcarbamoyl)-6-sulfanyl-hexyl]-5-oxo-pyrrolidine-2-carboxamide (**88**). ^1H NMR (300 MHz, $\text{DMSO-}d_6$) δ : 1.20–1.42 (m, 4H), 1.45–1.90 (m, 5H), 2.10–2.30 (m, 3H), 2.26 (s, 3H), 2.39–2.50 (m, 2H), 2.60 (s, 3H), 2.65 (m, 1H), 4.05–4.18 (m, 1H), 4.33–4.44 (m, 1H), 6.86 (d, $J = 7.6$ Hz, 1H), 7.17 (t, $J = 7.8$ Hz, 1H), 7.36 (d, $J = 8.3$ Hz, 1H), 7.41 (s, 1H), 8.46 (d, $J = 7.9$ Hz, 1H), 9.99 (s, 1H). ESI-MS m/z 392.2 (M + H) $^+$; 390.2 (M – H) $^-$.

(2*R*)-5-Oxo-*N*-[(1*S*)-6-Sulfanyl-1-[[3-(trifluoromethyl)phenyl]carbamoyl]hexyl]pyrrolidine-2-carboxamide (**89**). ^1H NMR (300 MHz, $\text{DMSO-}d_6$) δ : 1.20–1.43 (m, 4H), 1.45–1.97 (m, 5H), 2.00–2.35 (m, 4H), 2.39–2.50 (m, 2H), 4.06–4.14 (m, 1H), 4.34–4.45 (m, 1H), 7.40 (d, $J = 7.6$ Hz, 1H), 7.55 (t, $J = 8.0$ Hz, 1H), 7.78 (m, 2H), 7.80 (s, 1H), 8.09 (s, 1H), 8.23 (d, $J = 7.8$ Hz, 1H), 10.41 (s, 1H). ESI-MS m/z 432.1 (M + H) $^+$; 430.1 (M – H) $^-$.

((*S*)-1-Phenylcarbamoyl-hex-5-enyl)-carbamic acid *tert*-butyl ester (**54**) and compounds **57** and **90**–**95** were prepared from corresponding amines (the first step for route depicted in Scheme 4 is the same for route in Scheme 3, see above for synthesis and characterization).

(*S*)-2-Amino-hept-6-enoic Acid Phenylamide (**96**). To a stirred solution in DCM (20 mL) of ((*S*)-1-phenylcarbamoyl-hex-5-enyl)-carbamic acid *tert*-butyl ester **54** (76 mg, 0.35 mmol) at 0 °C was added TFA (4 mL) slowly. The reaction mixture was then allowed to warm to RT and stirred for 2 h. The solvent was removed under reduced pressure to afford the desired adduct quantitatively as the trifluoroacetate salt **96**, which was used without any purification in the next step.

Compounds **97**–**103** were prepared similarly from **57** and **90**–**95**.

(*R*)-6-Oxo-piperidine-2-carboxylic Acid ((*S*)-1-Phenylcarbamoyl-hex-5-enyl)-amide (**104**). A solution of DCM/DMF (10 mL, 10/2) of the trifluoroacetate salt was reacted with (*R*)-6-oxo-piperidine-2-carboxylic acid (263 mg, 0.79 mmol) and PyBOP (411 mg, 0.79 mmol) in the presence of NEt_3 (316 μL , 2.25 mmol) for 2 h. The reaction mixture was diluted with DCM and washed with 5% Na_2CO_3 , brine, 5% citric acid, and brine. The organic phase was dried over Na_2SO_4 , filtered, and concentrated under reduced pressure. The crude reaction mixture was purified through chromatography on silica gel using AcOEt/MeOH (9/1) as eluent to allow the desired adduct as a white solid **104** (85%). ^1H NMR (300 MHz, $\text{DMSO-}d_6$) δ : 1.28–1.50 (m, 2H), 1.52–1.78 (m, 5H), 1.80–1.95 (m, 1H), 1.97–2.08 (m, 2H), 2.11 (t, $J = 6.6$ Hz, 2H), 3.92–4.00 (m, 1H), 4.38–4.49 (m, 1H), 4.90–5.04 (m, 2H), 5.70–5.85 (m, 1H), 7.04 (t, $J = 7.5$ Hz, 1H), 7.29 (t, $J = 8.4$ Hz, 2H), 7.47 (d, $J = 2.6$ Hz, 1H), 7.57 (d, $J = 8.6$ Hz, 2H), 8.13 (d, $J = 8.1$ Hz, 1H), 10.03 (s, 1H). ESI-MS m/z 366.3 (M + Na) $^+$; 342.2 (M – H) $^-$.

Compounds **105**–**114** were prepared similarly from trifluoroacetate salts **96**–**103** and corresponding carboxylic acids.

Thioacetic Acid *S*-[(*S*)-6-[(*R*)-6-Oxo-piperidine-2-carbonyl]-amino]-6-phenylcarbamoyl-hexyl Ester (**115**). To a stirred solution of (*R*)-6-oxo-piperidine-2-carboxylic acid ((*S*)-1-phenylcarbamoyl-hex-5-enyl)-amide **104** (220 mg, 0.64 mmol), and thioacetic acid (460 μL , 6.4 mmol) at 75 °C in degassed dioxane (7 mL) was added AIBN (105 mg, 0.64 mmol). The reaction mixture was stirred until complete conversion of the starting material as monitored by TLC analysis. The reaction mixture was cooled to 0 °C and quenched with an excess of cyclohexene under stirring, the latter being maintained for 20 min. Concentration under reduced pressure and purification through chromatography on silica gel using hexane/DCM/IPA (50/40/10) as eluent afforded the desired adduct **115** (53%). ^1H NMR (300 MHz, $\text{DMSO-}d_6$) δ : 1.18–1.40 (m, 4H), 1.40–1.80 (m, 7H), 1.80–1.95 (m, 1H), 2.11 (t, $J = 6.6$ Hz, 2H), 2.29 (s, 3H), 2.79 (t, $J = 7.2$ Hz, 2H), 3.91–3.99 (m, 1H), 4.35–4.47 (m, 1H), 7.03 (t, $J = 7.5$ Hz, 1H), 7.29 (t, $J = 8.4$ Hz, 2H), 7.48 (d, $J = 2.4$ Hz, 1H), 7.57 (d, $J = 8.5$ Hz, 2H), 8.14 (d, $J = 8.2$ Hz, 1H), 10.05 (s, 1H). ESI-MS m/z 420.1 (M + H) $^+$; 532.2 (M + CF_3COO) $^-$.

Compounds **116**–**125** were prepared similarly from **105**–**114**.

Thioacetic Acid *S*-[(*S*)-6-[(*S*)-6-Oxo-piperidine-2-carbonyl]-amino]-6-phenylcarbamoyl-hexyl Ester (**116**). ^1H NMR (300 MHz, $\text{DMSO-}d_6$) δ : 1.20–1.40 (m, 4H), 1.41–1.87 (m, 8H), 2.10 (t, $J = 6.6$ Hz, 2H), 2.29 (s, 3H), 2.80 (t, $J = 7.1$ Hz, 2H), 3.90–4.01

(m, 1H), 4.30–4.45 (m, 1H), 7.04 (t, $J = 7.4$ Hz, 1H), 7.29 (t, $J = 8.2$ Hz, 2H), 7.49 (d, $J = 2.3$ Hz, 1H), 7.57 (d, $J = 7.7$ Hz, 2H), 8.11 (d, $J = 7.7$ Hz, 1H), 9.99 (s, 1H). ESI-MS m/z 420.0 (M + H)⁺; 532.2 (M + CF₃COO)⁻.

Thioacetic Acid S-[(S)-6-[(R)-5-Oxo-pyrrolidine-2-carbonyl]-amino]-6-phenylcarbamoyl-hexyl Ester (117). ¹H NMR (500 MHz, CD₃OD) δ : 1.20–1.40 (m, 4H), 1.41–1.76 (m, 4H), 1.77–1.91 (m, 1H), 1.99–2.34 (m, 3H), 2.29 (s, 3H), 2.79 (t, $J = 7.2$ Hz, 2H), 4.04–4.14 (m, 1H), 4.35–4.47 (m, 1H), 7.03 (t, $J = 7.3$ Hz, 1H), 7.28 (t, $J = 8.4$ Hz, 2H), 7.57 (d, $J = 7.6$ Hz, 2H), 7.80 (s, 1H), 8.19 (d, $J = 7.9$ Hz, 1H), 10.06 (s, 1H). ESI-MS m/z 428.17 (M + Na)⁺. HRMS (Orbitrap, ESI⁺): C₂₀H₂₇N₃O₄S, [M + Na]⁺: found 428.1602, calculated 428.1614. HRMS (Orbitrap, ESI⁻): C₂₀H₂₇N₃O₄S, [M - H]⁻: found 404.1656, calculated 404.1650.

S-[(6S)-7-Oxo-7-(phenylamino)-6-[(N-propanoyl-D-alanyl)-amino]heptyl] Ethanethioate (118). ¹H NMR (300 MHz, DMSO-*d*₆) δ : 0.97 (t, $J = 7.6$ Hz, 3H), 1.18 (d, $J = 7.1$ Hz, 3H), 1.20–1.40 (m, 4H), 1.40–1.78 (m, 4H), 2.11 (q, $J = 7.6$ Hz, 2H), 2.29 (s, 3H), 2.80 (t, $J = 7.1$ Hz, 2H), 4.19–4.40 (m, 2H), 7.03 (t, $J = 7.2$ Hz, 1H), 7.28 (t, $J = 7.9$ Hz, 2H), 7.60 (d, $J = 8.1$ Hz, 2H), 7.97 (d, $J = 7.1$ Hz, 2H), 9.86 (s, 1H). ESI-MS m/z 422.7 (M + H)⁺.

Thioacetic Acid S-[(S)-6-[(S)-6-Oxo-piperidine-2-carbonyl]-amino]-6-m-tolylcarbamoyl-hexyl Ester (119). ¹H NMR (300 MHz, DMSO-*d*₆) δ : 1.20–1.40 (m, 4H), 1.41–1.79 (m, 6H), 1.79–1.96 (m, 2H), 2.09 (t, $J = 6.7$ Hz, 2H), 2.25 (s, 3H), 2.29 (s, 3H), 2.79 (t, $J = 7.2$ Hz, 2H), 3.90–3.98 (m, 1H), 4.31–4.42 (m, 1H), 6.85 (d, $J = 7.5$ Hz, 1H), 7.16 (t, $J = 7.9$ Hz, 1H), 7.35 (d, $J = 7.8$ Hz, 1H), 7.40 (s, 1H), 7.47 (d, $J = 2.3$ Hz, 1H), 8.09 (d, $J = 7.8$ Hz, 1H), 9.90 (s, 1H). ESI-MS m/z 456.4 (M + H)⁺.

Thioacetic Acid S-[(S)-6-[(S)-6-Oxo-piperidine-2-carbonyl]-amino]-6-p-tolylcarbamoyl-hexyl Ester (120). ¹H NMR (300 MHz, DMSO-*d*₆) δ : 1.20–1.40 (m, 4H), 1.41–1.79 (m, 7H), 1.79–1.92 (m, 1H), 2.10 (t, $J = 6.6$ Hz, 2H), 2.23 (s, 3H), 2.29 (s, 3H), 2.79 (t, $J = 7.3$ Hz, 2H), 3.91–3.99 (m, 1H), 4.31–4.42 (m, 1H), 7.09 (d, $J = 8.2$ Hz, 2H), 7.41–7.49 (m, 3H), 8.06 (d, $J = 7.9$ Hz, 1H), 9.88 (s, 1H). ESI-MS m/z 456.6 (M + H)⁺.

9H-Fluoren-9-ylmethyl-4-[(2S)-7-(acetylsulfanyl)-2-[(6-oxopiperidin-2-yl)carbonyl]-amino]heptanoyl]amino]phenylpiperidine-1-carboxylate (121). ¹H NMR (300 MHz, DMSO-*d*₆) δ : 1.20–1.40 (m, 4H), 1.41–1.95 (m, 12H), 2.10 (t, $J = 6.6$ Hz, 2H), 2.28 (s, 3H), 2.55–2.70 (m, 1H), 2.70–2.92 (m, 4H), 3.80–4.15 (m, 3H), 4.24–4.33 (m, 1H), 4.34–4.55 (m, 3H), 6.89 (d, $J = 7.5$ Hz, 1H), 7.22 (t, $J = 7.8$ Hz, 1H), 7.30–7.51 (m, 7H), 7.62 (d, $J = 7.2$ Hz, 2H), 7.87 (d, $J = 6.6$ Hz, 2H), 8.07 (d, $J = 7.8$ Hz, 1H), 9.93 (s, 1H). ESI-MS m/z 725.4 (M + H)⁺; 837.3 (M + CF₃COO)⁻.

9H-Fluoren-9-ylmethyl-4-[(2S)-7-(acetylsulfanyl)-2-[(6-oxopiperidin-2-yl)carbonyl]-amino]heptanoyl]amino]phenylpiperidine-1-carboxylate (122). ¹H NMR (300 MHz, DMSO-*d*₆) δ : 1.20–1.40 (m, 6H), 1.42–1.93 (m, 10H), 2.10 (t, $J = 6.6$ Hz, 2H), 2.29 (s, 3H), 2.50–2.68 (m, 1H), 2.69–2.90 (m, 4H), 3.75–4.15 (m, 3H), 4.20–4.55 (m, 4H), 7.12 (d, $J = 8.4$ Hz, 2H), 7.29–7.45 (m, 4H), 7.46–7.53 (m, 3H), 7.63 (d, $J = 7.2$ Hz, 2H), 7.87 (d, $J = 7.2$ Hz, 2H), 8.08 (d, $J = 7.5$ Hz, 1H), 9.93 (s, 1H). ESI-MS m/z 725.4 (M + H)⁺; 837.3 (M + CF₃COO)⁻.

Thioacetic Acid S-[(S)-6-[(S)-6-Oxo-piperidine-2-carbonyl]-amino]-6-(4-trifluoromethyl-benzylcarbamoyl)-hexyl Ester (123). ¹H NMR (500 MHz, CD₂Cl₂) δ : 1.30–1.47 (m, 4H), 1.52–1.62 (m, 2H), 1.64–1.94 (m, 5H), 2.00–2.10 (m, 1H), 2.17–2.30 (m, 2H), 2.32 (s, 3H), 2.84 (t, $J = 7.0$ Hz, 2H), 3.95–4.05 (m, 1H), 4.40–4.51 (m, 3H), 7.16–7.25 (m, 1H), 7.30–7.47 (m, 4H), 7.57–7.64 (m, 2H). ESI-MS m/z 502.1 (M + H)⁺.

Thioacetic Acid S-[(S)-6-(3-Benzyloxy-benzylcarbamoyl)-6-[(S)-6-oxo-piperidine-2-carbonyl]-amino]-hexyl Ester (124). ¹H NMR (500 MHz, CD₂Cl₂) δ : 1.25–1.45 (m, 4H), 1.50–1.60 (m, 2H), 1.62–1.95 (m, 5H), 1.97–2.07 (m, 1H), 2.15–2.30 (m, 2H), 2.30 (s, 3H), 2.83 (t, $J = 7.1$ Hz, 2H), 3.95–4.01 (m, 1H), 4.30–4.42 (m, 2H), 4.42–4.50 (m, 1H), 5.06 (m, 2H), 6.82–6.92 (m, 3H), 6.97–7.07 (m, 1H), 7.24 (t, $J = 7.8$ Hz, 1H), 7.32–7.50 (m, 5H). ESI-MS m/z 540.2 (M + H)⁺.

Thioacetic Acid S-[(S)-6-[(S)-6-Oxo-piperidine-2-carbonyl]-amino]-6-cyclopentylcarbamoyl-hexyl Ester (125). ¹H NMR (300

MHz, DMSO-*d*₆) δ : 1.10–1.90 (m, 20H), 2.10 (t, $J = 6.5$ Hz, 2H), 2.30 (s, 3H), 2.79 (t, $J = 7.1$ Hz, 2H), 3.86–4.02 (m, 2H), 4.13–4.24 (m, 1H), 7.50 (d, $J = 2.5$ Hz, 1H), 7.82 (s, 1H), 7.84 (s, 1H). ESI-MS m/z 434.4 (M + Na)⁺.

(R)-6-Oxo-piperidine-2-carboxylic Acid [(S)-6-Mercapto-1-phenylcarbamoyl-hexyl]-amide (126). To a stirred solution of thioacetate **115** (420 mg, 1 mmol) in methanol (10 mL) under nitrogen at 23 °C was added sodium thiomethoxide (70 mg, 1 equiv 1 M solution in MeOH). The reaction mixture was stirred at 23 °C for 30 min. The solution was then added to aqueous HCl 20 mL/0.1M. The aqueous solution was extracted with CH₂Cl₂. The combined organic layers were washed with brine, dried over MgSO₄, filtered, and concentrated to obtain compound **126** which was purified through HPLC (27%). ¹H NMR (300 MHz, DMSO-*d*₆) δ : 1.18–1.42 (m, 4H), 1.45–1.79 (m, 7H), 1.80–1.95 (m, 1H), 2.11 (t, $J = 6.4$ Hz, 2H), 2.22 (t, $J = 7.9$ Hz, 1H), 2.38–2.49 (m, 2H), 3.90–4.01 (m, 1H), 4.38–4.48 (m, 1H), 7.04 (t, $J = 7.4$ Hz, 1H), 7.29 (t, $J = 8.2$ Hz, 2H), 7.49 (d, $J = 2.3$ Hz, 1H), 7.57 (d, $J = 7.6$ Hz, 2H), 8.13 (d, $J = 8.0$ Hz, 1H), 10.04 (s, 1H). ESI-MS m/z 400.2 (M + Na)⁺; 376.2 (M - H)⁻.

Compounds **127–133** were prepared from the corresponding thioacetates **116–117**, **119–120**, and **123–125**.

(S)-6-Oxo-piperidine-2-carboxylic Acid [(S)-6-Mercapto-1-phenylcarbamoyl-hexyl]-amide (127). ¹H NMR (300 MHz, DMSO-*d*₆) δ : 1.20–1.42 (m, 4H), 1.45–1.80 (m, 7H), 1.80–1.95 (m, 1H), 2.10 (t, $J = 6.5$ Hz, 2H), 2.21 (t, $J = 7.1$ Hz, 1H), 2.37–2.50 (m, 2H), 3.92–4.02 (m, 1H), 4.33–4.47 (m, 1H), 7.04 (t, $J = 7.4$ Hz, 1H), 7.29 (t, $J = 8.2$ Hz, 2H), 7.49 (d, $J = 2.3$ Hz, 1H), 7.58 (d, $J = 7.6$ Hz, 2H), 8.10 (d, $J = 7.9$ Hz, 1H), 9.99 (s, 1H). ESI-MS m/z 400.4 (M + Na)⁺; 376.3 (M - H)⁻.

(R)-5-Oxo-pyrrolidine-2-carboxylic Acid [(S)-6-Mercapto-1-phenylcarbamoyl-hexyl]-amide (128). ¹H NMR (300 MHz, DMSO-*d*₆) δ : 1.20–1.45 (m, 4H), 1.46–1.93 (m, 5H), 2.00–2.39 (m, 4H), 2.40–2.5 (m, 2H), 4.08–4.17 (m, 1H), 4.37–4.49 (m, 1H), 7.05 (t, $J = 7.4$ Hz, 1H), 7.31 (t, $J = 7.4$ Hz, 2H), 7.59 (d, $J = 7.6$ Hz, 2H), 7.83 (s, 1H), 8.19 (d, $J = 8.1$ Hz, 1H), 10.07 (s, 1H). ESI-MS m/z 364.3 (M + H)⁺. HRMS (Orbitrap, ESI⁺): C₁₈H₂₅N₃O₃S, [M + Na]⁺: found 386.1509, calculated 386.1509. HRMS (Orbitrap, ESI⁻): C₁₈H₂₅N₃O₃S, [M - H]⁻: found 362.1548, calculated 362.1544.

(S)-6-Oxo-piperidine-2-carboxylic Acid [(S)-6-Mercapto-1-m-tolylcarbamoyl-hexyl]-amide (129). ¹H NMR (300 MHz, DMSO-*d*₆) δ : 1.20–1.41 (m, 4H), 1.44–1.91 (m, 8H), 2.10 (t, $J = 6.7$ Hz, 2H), 2.20 (t, $J = 7.9$ Hz, 1H), 2.26 (s, 3H), 2.39–2.47 (m, 2H), 3.92–3.99 (m, 1H), 4.32–4.43 (m, 1H), 6.85 (d, $J = 7.3$ Hz, 1H), 7.16 (t, $J = 7.9$ Hz, 1H), 7.36 (d, $J = 7.9$ Hz, 1H), 7.41 (s, 1H), 7.48 (d, $J = 2.6$ Hz, 1H), 8.06 (d, $J = 7.9$ Hz, 1H), 9.89 (s, 1H). ESI-MS m/z 414.3 (M + Na)⁺; 390.4 (M - H)⁻.

(S)-6-Oxo-piperidine-2-carboxylic Acid [(S)-6-Mercapto-1-p-tolylcarbamoyl-hexyl]-amide (130). ¹H NMR (500 MHz, DMSO-*d*₆) δ : 1.33 (m, 4H), 1.51 (m, 2H), 1.60 (m, 5H), 1.83 (m, 1H), 2.10 (t, $J = 6.6$ Hz, 2H), 2.21 (t, $J = 7.0$ Hz, 1H), 2.23 (s, 3H), 2.40–2.49 (m, 2H), 3.91–3.90 (m, 1H), 4.33–4.42 (m, 1H), 7.09 (d, $J = 8.4$ Hz, 2H), 7.45 (d, $J = 8.2$ Hz, 2H), 7.48 (s, 1H), 8.08 (d, $J = 7.9$ Hz, 1H), 9.89 (s, 1H). ESI-MS m/z 414.4 (M + Na)⁺; 390.3 (M - H)⁻.

(S)-6-Oxo-piperidine-2-carboxylic Acid [(S)-6-Mercapto-1-(4-trifluoromethyl-benzylcarbamoyl)-hexyl]-amide (131). ¹H NMR (500 MHz, CD₂Cl₂) δ : 1.38 (m, 5H), 1.52–2.12 (m, 8H), 2.18–2.28 (m, 2H), 2.45–2.56 (m, 2H), 3.94–4.03 (m, 1H), 4.34–4.53 (m, 3H), 7.20 (t, $J = 5.7$ Hz, 1H), 7.38 (d, $J = 7.8$ Hz, 3H), 7.48 (s, 1H), 7.58 (d, $J = 8.1$ Hz, 2H). ESI-MS m/z 460.1 (M + H)⁺.

(S)-6-Oxo-piperidine-2-carboxylic Acid [(S)-1-(3-Benzyloxy-benzylcarbamoyl)-6-mercapto-hexyl]-amide (132). ¹H NMR (500 MHz, CD₂Cl₂) δ : 1.24–1.46 (m, 5H), 1.54–2.02 (m, 8H), 2.13–2.30 (m, 2H), 2.45–3.53 (m, 2H), 3.91–3.97 (m, 1H), 4.25–4.43 (m, 2H), 4.47–4.55 (m, 1H), 5.04 (s, 2H), 6.81–6.91 (m, 3H), 7.23 (t, $J = 7.9$ Hz, 1H), 7.32–7.38 (m, 2H), 7.38–7.47 (m, 3H), 7.64 (s, 1H), 7.75 (d, $J = 8.2$ Hz, 1H). ESI-MS m/z 498.4 (M + H)⁺.

(S)-6-Oxo-piperidine-2-carboxylic Acid [(S)-1-Cyclopentylcarbamoyl-6-mercapto-hexyl]-amide (133). ¹H NMR (500 MHz, DMSO-*d*₆) δ : 1.10–1.90 (m, 20H), 2.12 (t, $J = 6.4$ Hz, 2H), 2.21 (t, $J = 7.9$ Hz, 1H), 2.40–2.50 (m, 2H), 3.88–4.02 (m, 2H), 4.18–4.28 (m, 1H),

7.55 (d, $J = 2.3$ Hz, 1H), 7.80 (s, 1H), 7.82 (s, 1H). ESI-MS m/z 392.2 (M + Na)⁺; 368.1 (M - H)⁻.

Ethyl [(6S)-7-Anilino-7-oxo-6-[[[(2R)-5-oxopyrrolidine-2-carbonyl]amino]heptyl]sulfanylformate (134). To a solution of (R)-5-oxo-pyrrolidine-2-carboxylic acid ((S)-6-mercapto-1-phenylcarbamoyl-hexyl)-amide **128** (76 mg, 0.21 mmol) in DCM (20 mL) were added NEt₃ (32 μ L, 0.23 mmol) and ethylchloroformate (22 μ L, 0.23 mmol). The reaction mixture was stirred at RT for 2 h. The reaction mixture was concentrated under reduced pressure, and the crude product was purified through chromatography on silica gel using AcOEt/MeOH 80/20 as eluent to obtain the compound **134** (74%). ¹H NMR (300 MHz, DMSO-*d*₆) δ : 1.19 (t, $J = 7.0$ Hz, 3H), 1.25–1.45 (m, 4H), 1.45–1.95 (m, 5H), 2.00–2.35 (m, 3H), 2.80 (t, $J = 7.3$ Hz, 2H), 4.05–4.11 (m, 1H), 4.16 (q, $J = 7.0$ Hz, 2H), 4.35–4.48 (m, 1H), 7.03 (t, $J = 7.3$ Hz, 1H), 7.28 (t, $J = 8.2$ Hz, 2H), 7.57 (d, $J = 7.6$ Hz, 2H), 7.81 (s, 1H), 8.18 (d, $J = 8.2$ Hz, 1H), 10.05 (s, 1H). ESI-MS m/z 436.2 (M + H)⁺.

Compounds **135–136** were prepared similarly from **128** and isobutryl chloride and ethylchloroformate, respectively.

Thioisobutyric Acid S-[(S)-6-[(S)-6-Oxo-piperidine-2-carbonyl]-amino]-6-phenylcarbamoyl-hexyl Ester (135). ¹H NMR (500 MHz, DMSO-*d*₆) δ : 1.00–1.07 (m, 6H), 1.22–1.44 (m, 4H), 1.46–1.77 (m, 6H), 1.88–1.97 (m, 1H), 2.02–2.10 (m, 1H), 2.20 (t, $J = 7.6$ Hz, 1H), 2.34–2.41 (m, 1H), 2.43–5.4 (m, 4H), 3.42–3.52 (m, 1H), 4.28–4.36 (m, 1H), 4.79–4.85 (m, 1H), 7.04 (t, $J = 7.3$ Hz, 1H), 7.29 (t, $J = 8.2$ Hz, 2H), 7.58 (d, $J = 7.6$ Hz, 2H), 8.33 (d, $J = 7.6$ Hz, 1H), 9.99 (s, 1H). ESI-MS m/z 448.2 (M + H)⁺.

Thiocarbonic Acid Ethyl Ester [(S)-6-[(S)-6-Oxo-piperidine-2-carbonyl]-amino]-6-phenylcarbamoyl-hexyl Ester (136). ¹H NMR (500 MHz, DMSO-*d*₆) δ : 1.20 (t, $J = 7.0$ Hz, 3H), 1.25–1.45 (m, 4H), 1.52–1.80 (m, 7H), 1.83–1.93 (m, 1H), 2.11 (t, $J = 6.5$ Hz, 2H), 2.82 (t, $J = 7.0$ Hz, 2H), 3.88–4.01 (m, 1H), 4.21 (q, $J = 7.1$ Hz, 2H), 4.35–4.45 (m, 1H), 7.05 (t, $J = 7.5$ Hz, 1H), 7.30 (t, $J = 8.0$ Hz, 2H), 7.48 (d, $J = 2.5$ Hz, 1H), 7.58 (d, $J = 8.0$ Hz, 2H), 8.10 (d, $J = 7.5$ Hz, 1H), 9.99 (s, 1H). ESI-MS m/z 450.1 (M + H)⁺.

(2S,2'S)-N,N'-[Disulfanediy]bis[(2S)-1-oxo-1-(phenylamino)-heptane-7,2-diy]bis(6-oxopiperidine-2-carboxamide) (137). A 2N solution of NaOH (343 mg, 7.0 mmol) was added to a solution of thioacetic acid S-[(S)-6-[(S)-6-oxo-piperidine-2-carbonyl]-amino]-6-phenylcarbamoyl-hexyl ester **116** (399 mg, 0.95 mmol) in EtOH (13 mL). The reaction mixture was stirred at RT overnight and then poured into water and extracted with AcOEt, washed with water and brine, and finally dried over Na₂SO₄. Removal of the solvent under reduced pressure led to the desired adduct as a side product **137** (20%), which was purified through HPLC. ¹H NMR (300 MHz, DMSO-*d*₆) δ : 1.18–1.93 (m, 24H), 2.09 (t, $J = 6.5$ Hz, 4H), 2.65 (t, $J = 7.0$ Hz, 4H), 3.90–4.01 (m, 2H), 4.30–4.43 (m, 2H), 7.04 (t, $J = 7.3$ Hz, 2H), 7.28 (t, $J = 8.0$ Hz, 4H), 7.51 (m, 2H), 7.59 (d, 4H), 8.35 (d, $J = 7.7$ Hz, 2H), 10.13 (s, 2H). ESI-MS m/z 753.4 (M + H)⁺.

[(R)-1-Phenylcarbamoyl-hex-5-enyl]-carbamic Acid tert-Butyl Ester (138). A solution of (R)-2-tert-butoxycarbonylamino-hept-6-enoic acid (292 mg, 2.05 mmol), DIPEA (1.07 mL, 6.15 mmol), and aniline (205 μ L, 2.25 mmol) was stirred at RT in DCM (30 mL) for 20 min before adding PyBOP (1.07 g, 2.05 mmol) and anhydrous DMF (2 mL). The reaction mixture was stirred for 2 h at RT. The solvent was removed under reduced pressure, and the crude reaction mixture was diluted with AcOEt, washed with 5% Na₂CO₃, water, and then with 5% aqueous citric acid and finally with brine. After removal of the solvent under reduced pressure and purification on silica gel (*n*-hexane/AcOEt 9/1), the desired adduct **138** was obtained (83%). ¹H NMR (300 MHz, DMSO-*d*₆) δ : 1.25–1.50 (m, 11H), 1.50–1.71 (m, 2H), 1.97–2.07 (m, 2H), 4.00–4.11 (m, 1H), 4.87–5.05 (m, 2H), 5.70–5.85 (m, 1H), 7.03 (m, $J = 7.4$ Hz, 2H), 7.29 (t, $J = 8.3$ Hz, 2H), 7.58 (d, $J = 7.6$ Hz, 2H), 9.93 (s, 1H). ESI-MS m/z 341.1 (M + Na)⁺.

(R)-2-Amino-hept-6-enoic Acid Phenylamide (139). To a stirred solution of ((R)-1-phenylcarbamoyl-hex-5-enyl)-carbamic acid tert-butyl ester at 0 °C was added TFA slowly. The reaction mixture was then allowed to warm to RT and stirred for 2 h. The solvent was removed under reduced pressure to afford the desired adduct

quantitatively as the trifluoroacetate salt **139**, which was used without any purification in the next step.

(2S)-6-Oxo-N-[(1R)-1-(phenylcarbamoyl)hex-5-enyl]piperidine-2-carboxamide (140). A solution of DCM/DMF (45 mL, 8/1) of the trifluoroacetate salt **139** was reacted with (R)-6-oxo-piperidine-2-carboxylic acid (1.78 mmol) and PyBOP (1.78 mmol) in the presence of DIPEA (16.2 mmol) for 2 h. The reaction mixture was diluted with DCM and washed with 5% Na₂CO₃, brine, 5% citric acid, and brine. The organic phase was dried over Na₂SO₄, filtered, and concentrated under reduced pressure. The crude reaction mixture was purified through chromatography on silica gel using AcOEt/MeOH (9/1) as eluent to allow the desired adduct as a white solid **140** (80%). ¹H NMR (300 MHz, DMSO-*d*₆) δ : 1.27–1.52 (m, 2H), 1.52–1.79 (m, 5H), 1.80–1.95 (m, 1H), 1.95–2.15 (m, 4H), 3.92–4.00 (m, 1H), 4.35–4.48 (m, 1H), 4.90–5.04 (m, 2H), 5.70–5.83 (m, 1H), 7.04 (t, $J = 7.3$ Hz, 1H), 7.30 (t, $J = 8.1$ Hz, 2H), 7.49 (s, 1H), 7.58 (d, $J = 8.0$ Hz, 2H), 8.14 (d, $J = 8.2$ Hz, 1H), 10.05 (s, 1H). ESI-MS m/z 366.3 (M + Na)⁺; 342.2 (M - H)⁻.

Compound **141** was prepared similarly from **139** and (2R)-5-oxopyrrolidine-2-carboxylic acid.

S-[(6R)-7-Anilino-7-oxo-6-[(2S)-6-oxopiperidine-2-carbonyl]-amino]heptyl Ethanethioate (142). To a stirred solution of (2S)-6-oxo-N-[(1R)-1-(phenylcarbamoyl)hex-5-enyl]piperidine-2-carboxamide **140** (343 mg, 1.0 mmol) and thioacetic acid (715 μ L, 10.0 mmol) at 75 °C in degassed dioxane (40 mL) was added AIBN (328 mg, 0.5 mmol). The reaction mixture was stirred until complete conversion of the starting material as monitored by TLC analysis. The reaction mixture was cooled to 0 °C and quenched with an excess of cyclohexene under stirring, the latter being maintained for 20 min. Concentration under reduced pressure and purification through chromatography on silica gel using hexane/DCM/IPA 50/40/10 as eluent afforded the desired adduct **142** (50%). ¹H NMR (300 MHz, DMSO-*d*₆) δ : 1.20–1.40 (m, 4H), 1.40–1.53 (m, 2H), 1.53–1.78 (m, 5H), 1.78–1.95 (m, 1H), 2.12 (t, $J = 6.4$ Hz, 2H), 2.30 (s, 3H), 2.79 (t, $J = 7.1$ Hz, 2H), 3.92–4.00 (m, 1H), 4.35–4.47 (m, 1H), 7.04 (t, $J = 7.4$ Hz, 1H), 7.30 (t, $J = 8.1$ Hz, 2H), 7.49 (d, $J = 2.4$ Hz, 1H), 7.57 (d, $J = 7.7$ Hz, 2H), 8.13 (d, $J = 8.0$ Hz, 1H), 10.04 (s, 1H). ESI-MS m/z 420.1 (M + H)⁺; 532.2 (M + CF₃COO)⁻.

Compound **143** was prepared similarly from **141**.

(2R)-5-Oxo-N-[(1R)-1-(phenylcarbamoyl)-6-sulfanyl-hexyl]-pyrrolidine-2-carboxamide (143). ¹H NMR (300 MHz, DMSO-*d*₆) δ : 1.20–1.40 (m, 4H), 1.41–1.80 (m, 4H), 1.80–1.95 (m, 1H), 2.00–2.32 (m, 3H), 2.30 (s, 3H), 2.80 (t, $J = 7.2$ Hz, 2H), 4.06–4.13 (m, 1H), 4.32–4.43 (m, 1H), 7.04 (t, $J = 7.4$ Hz, 1H), 7.29 (t, $J = 8.3$ Hz, 2H), 7.58 (d, $J = 7.6$ Hz, 2H), 7.79 (s, 1H), 8.21 (d, $J = 7.9$ Hz, 1H), 10.06 (s, 1H). ESI-MS m/z 428.1 (M + H)⁺.

(2S)-6-Oxo-N-[(1R)-1-(phenylcarbamoyl)-6-sulfanyl-hexyl]-piperidine-2-carboxamide (144). To a stirred solution of thioacetate **142** (101 mg, 0.24 mmol) in methanol (2 mL) under nitrogen at 23 °C was added sodium thiomethoxide (71 mg, 1 equiv 1 M solution in MeOH). The reaction mixture was stirred at 23 °C for 30 min. The solution was then added to aqueous HCl 4 mL/0.1M). The aqueous solution is extracted with CH₂Cl₂. The combined organic layers were washed with brine, dried over MgSO₄, filtered, and concentrated to obtain the compound **144**, which was purified through HPLC (25%). ¹H NMR (300 MHz, DMSO-*d*₆) δ : 1.20–1.45 (m, 4H), 1.45–1.80 (m, 7H), 1.80–1.97 (m, 1H), 2.12 (t, $J = 6.4$ Hz, 2H), 2.22 (t, $J = 7.6$ Hz, 1H), 2.37–2.50 (m, 2H), 3.92–4.00 (m, 1H), 4.38–4.48 (m, 1H), 7.04 (t, $J = 7.2$ Hz, 1H), 7.30 (t, $J = 7.9$ Hz, 2H), 7.49 (d, $J = 2.3$ Hz, 1H), 7.58 (d, $J = 8.0$ Hz, 2H), 8.13 (d, $J = 8.2$ Hz, 1H), 10.04 (s, 1H). ESIMS m/z 400.1 (M + Na)⁺.

Compound **145** was prepared similarly from **143**.

(2R)-5-Oxo-N-[(1R)-1-(phenylcarbamoyl)-6-sulfanyl-hexyl]-pyrrolidine-2-carboxamide (145). ¹H NMR (300 MHz, DMSO-*d*₆) δ : 1.20–1.40 (m, 4H), 1.45–1.79 (m, 4H), 1.80–1.94 (m, 1H), 1.97–2.12 (m, 3H), 2.40–2.50 (m, 2H), 4.05–4.13 (m, 1H), 4.32–4.44 (m, 1H), 7.04 (t, $J = 7.4$ Hz, 1H), 7.29 (t, $J = 8.3$ Hz, 2H), 7.58 (d, $J = 8.1$ Hz, 2H), 7.79 (s, 1H), 8.18 (d, $J = 7.8$ Hz, 1H), 10.04 (s, 1H). ESI-MS m/z 364.0 (M + H)⁺.

HDAC Inhibition Assay. The newly synthesized thiol derivatives reported in Tables 1 and 2 were evaluated for their activity against class I (1–3, 8), IIa (4, 5, 7, 9), IIb (6, 11), and IV (11) HDAC isoforms. HDAC profiling was performed in the presence of a 50 μ M solution of the fluorogenic tetrapeptide RHKK(Ac) substrate (from p53 residues 379–382) for all isoforms, with the exception of HDAC8, which was assayed in the presence of a 50 μ M solution of its diacetylated analogue RHK(Ac)K(Ac). Class IIa isoforms were assayed either applying the standard substrate or in the presence of a 50 μ M solution of the fluorogenic Boc-Lys(trifluoroacetyl)-AMC (Supporting Information Table S2).³⁶

Cell Culture. HCT116 (human colon carcinoma) and NCI-H460 (human nonsmall cell lung carcinoma) cells were obtained from American Type Culture Collection and were grown, respectively, in McCoy's 5A and RPMI-1640 medium containing L-glutamine and supplemented with 10% heat-inactivated fetal calf serum (FCS, Life Technologies) and 50 μ g/mL gentamicin.

Cell Proliferation Assay. HCT-116 and NCI-H460 tumor cell lines were grown in a volume of 200 μ L, at approximately 10% confluence, in 96-well Multi-Tier plates and were allowed to recover for an additional 24 h. Tumor cells were treated with either varying concentrations of drugs or solvent for 24 h. After treatment, the plates were washed to remove drug and incubated for further other 48 h. The fraction of cells surviving after compound treatment was determined using the SRB assay.³⁷ IC₅₀ was defined as the drug concentration causing a 50% reduction in cell number compared with that of vehicle-treated cells and was calculated by the "ALLFIT" computer program by analyzing dose–response inhibition curves.

Western Blot Analysis for H4-Histone and α -Tubulin Acetylation. The day before the experiment NCI-H460 NSCLC cells were plated in complete culture medium. Cells were then treated for 3 h with test compounds at various concentrations (dose–response curves), depending on their relative potency. Compound 1 was used as reference inhibitor. After treatment cells were washed twice with DPBS supplemented with 5 mM NaB and then were collected and resuspended in HNB buffer (0.5 M sucrose, 15 mM Tris/HCl pH 7.5, 60 mM KCl, 0.25 mM EDTA pH 8, 0.125 mM EGTA pH 8, 0.5 mM spermidine, 0.15 mM spermine, 1 mM DTT, 0.5 mM PMSF, 5 μ g/mL pepstatin, 5 μ g/mL leupeptin, 5 μ g/mL aprotinin) supplemented with 1% NP-40. After 5 min of incubation at 4 $^{\circ}$ C, nuclei were isolated by centrifugation at 2000g for 3 min. Cytoplasm proteins isolated at this step were collected and then separated on SDS-PAGE for the analysis of α -tubulin acetylation.

Histones, acid soluble proteins, were isolated from nuclei by addition of 0.4 equiv/L H₂SO₄ and incubation at 4 $^{\circ}$ C for 1 h. After centrifugation, histones were precipitated from the supernatant by addition of prechilled acetone and incubation overnight at –20 $^{\circ}$ C and then air-dried. After solvent removal, proteins were resuspended in distilled water, and the protein content was determined by the classical colorimetric Bradford method (Coomassie Bradford protein assay kit; Pierce, cat. 23200), according to the manufacturer's instruction.

To assess the extent of acetylation, equal amounts of histones or cytoplasmic proteins for each sample were resolved by SDS-PAGE and transferred onto a nitrocellulose membrane (Hybond-C extra, Amersham-GE Healthcare). Molecular weights were estimated based upon the relative migration with molecular weight protein markers (Prestained Kaleidoscope Standards; cat. 161-0324, Bio-Rad). Non-specific binding sites were then blocked by incubation of the membranes with 5% nonfat dry milk in TBS, overnight at 4 $^{\circ}$ C. Specific primary antibodies (rabbit antiacetyl-histone H4 polyclonal antibody, cat. 06-598, and mouse anti-histone H4 monoclonal antibody, cat. 07-108, from Upstate; mouse antiacetylated α -tubulin monoclonal antibody, cat. T6793, mouse anti- α -tubulin monoclonal antibody, cat. T5168, and mouse anti- β -actin monoclonal antibody, cat. A5316, from Sigma), were added to the membranes at the optimal dilution in 5% nonfat dry milk/TBST overnight at 4 $^{\circ}$ C. Following four washes in TBST, membranes were incubated for 1 h with HRP-conjugated secondary antibodies in 5% nonfat dry milk/TBST. Immunoreactive bands were finally visualized by enhanced chemiluminescence with the ECLplus Western blotting detection reagent

(GE Healthcare) and analyzed by a phosphoimaging system (STORM, Molecular Dynamics). Following densitometry analysis and normalization, the IC₅₀ values were finally calculated by the "ALLFIT" computer program.

Plasma Stability. Test compounds were added to human plasma to get a final concentration of 5 μ M and incubated at 37 $^{\circ}$ C at different times (until 120 min). Then 0.1 mL of each sample was taken, added in a corresponding 2-fold amount of chilled acetonitrile, and centrifuged at +4 $^{\circ}$ C. The supernatant was then submitted to LC-MS/MS analysis. At the end of incubation, % of intact compound remaining was calculated.

Animals. In vivo experiments were carried out using female athymic nude mice, 5–6 weeks old (Harlan). Mice were maintained in laminar flow rooms keeping temperature and humidity constant. Mice had free access to food and water. Experiments were approved by the Ethics Committee for Animal Experimentation of Sigma-Tau according to institutional guidelines.

Xenograft Tumor Models. For subcutaneous (sc) tumor model, exponentially growing tumor cells (5 \times 10⁶/100 μ L) were sc inoculated in the right flank of nude mice. Mice were treated starting 3 days after tumor injection. Tumor volume (TV) was calculated according to the formula: TV (mm³) = $d^2 \times D/2$ where d and D are the shortest and the longest diameter, respectively. HDAC inhibitors were delivered by oral route according to the schedule qdx5/wx3w or qdx5/wx2w. Carboplatin was given intraperitoneally according to the schedule q4d/wx3w. Compound 1 was administered by oral route according to the schedule qdx5w/x2w. Drug efficacy was assessed as tumor volume inhibition percentage (TVI%) in drug-treated versus control mice, expressed as TVI% = 100 – [(mean TV treated/mean TV control) \times 100]. Toxic effects of the drug treatment were assessed as body weight loss percentage (BWL%), calculated as BWL% = 100 – [(mean BW day x /mean BW day 1) \times 100], where day 1 was the first day of treatment and day x was any day thereafter. The highest (max) BWL% is reported in Table 6.

Molecular Modeling. Molecular modeling studies were conducted with the Schrodinger software suite. Ligand molecules were built in Maestro 9.6³⁸ and prepared with Ligprep 2.8,³⁹ while protein structures were refined using the Protein Preparation Wizard.⁴⁰ Docking studies were carried out with Glide 6.1^{41,42} using the SP scoring function. Default settings were used, unless stated otherwise.

Protein Preparation. The crystal structures of human HDAC3 (PDB 4A69⁴³ (chain B)) and HDAC8 (PDB 2V5X⁴⁴ (chain A)) were used for docking studies. The protein C- and N-termini were capped with acetyl and methylamino groups, respectively, and missing hydrogen atoms were added. The overall hydrogen bonding network was optimized by sampling the orientations of hydroxyl and thiol groups, the conformations of asparagine, glutamine, and histidine side chains and by adjusting the protonation state of glutamate and aspartate residues. At the end of the protein preparation, all histidine residues were in their neutral form except for H142 in HDAC8 and H134 in HDAC3 which were protonated. Zero-order bonds connecting the potassium and zinc ions to their coordinating atoms were built. The resulting structures were submitted to a first energy minimization procedure with the OPLS2005 force field⁴⁵ in which only hydrogen atoms were free to move. A second minimization run was then performed on all atoms, restraining the positions of protein heavy atoms until a root-mean-square deviation (RMSD) value of 0.3 Å was reached. All crystallized water molecules were removed before docking studies.

Docking Calculations. Glide grids were built with Glide 6.1 and were centered on the acetate and inhibitor molecules cocrystallized with HDAC3 and HDAC8, respectively. The dimensions of bounding and enclosing boxes were set to 16 and 31 Å , respectively; no van der Waals scaling was applied to nonpolar protein atoms. The zinc ion in HDAC8 adopts a tetrahedral coordination geometry to interact with the thiolate group of the cocrystallized inhibitor.⁴⁶ For this reason, a positional constraint was applied during grids generation to force the thiol group of docked compounds to occupy the free coordination site of the tetrahedrally coordinated zinc ion. Ligands were initially prepared with Ligprep 2.8³⁹ to generate suitable protonation states and

were then subjected to energy minimization with Macromodel 10.2,⁴⁷ applying the OPLS2005 force field to an energy gradient of 0.05 kJ mol⁻¹ Å⁻¹. 100 Poses were collected for each docking run and subsequently ranked according to their Emodel values. The top-ranked pose for each ligand was retained and further analyzed.

To allow the accommodation of the benzyloxy-benzyl substituent of compound **132** in the rim of HDAC8 structure, the side chain of K33 which occludes the binding site was rotated in the same conformation as that observed in another HDAC8 crystal structure, in complex with a hydroxamate-based inhibitor (PDB 3F07).⁴⁸

Molecular Dynamics (MD) Simulations. The best-ranked HDAC3-127 and HDAC3-144 complexes obtained from molecular docking were submitted to MD simulations. The cocrystallized water molecules removed prior to docking studies were reintroduced. Resulting complexes were then solvated with ~11600 TIP3P water molecules in a box of 75 × 72 × 79 Å³ and neutralized by adding 7 sodium ions. Systems were first equilibrated for 3 ns using a modified version of the relaxation protocol implemented in Desmond 3.6.^{49,50} The equilibration phase was followed by 20 ns long MD simulations performed at 310 K and 1 atm in the NPT ensemble applying the Langevin coupling scheme⁵¹ and the OPLS2005 force field. The M-SHAKE algorithm⁵² was applied to constrain all bond lengths to hydrogen atoms. Long-range electrostatic interactions were calculated by applying the Smooth Particle Mesh Ewald method,⁵³ while short-range electrostatic interactions were cut off at 9 Å. A RESPA integrator⁵⁴ was used with a time-step of 2 fs, and long-range electrostatics were computed every 6 fs. Three independent simulations were conducted for each system using different initial random velocity seeds.

■ ASSOCIATED CONTENT

● Supporting Information

List of all mentioned compounds; inhibitory activity (IC₅₀) on class IIa HDAC isoforms; distances monitored during molecular dynamics simulations; stability and solubility of thiol prodrugs; cytotoxicity of thiol prodrugs; selectivity profiles for compounds **117** and **128**; vehicle selection for oral administration; HRMS for compound **117**; NMR and mass spectra of selected compounds. This material is available free of charge via the Internet at <http://pubs.acs.org>.

■ AUTHOR INFORMATION

Corresponding Author

*Phone: +39-0691394441. Fax: +39-0691393638. E-mail: giuseppe.giannini@sigma-tau.it.

Present Addresses

^{||}For C.P.: Biogem SCARL, Via Camporeale, I-83031 Ariano Irpino (AV), Italy.

[†]For W.C.: Fresenius Kabi, Piazza Maestri del Lavoro 7, I-20063 Cernusco sul Naviglio (MI), Italy.

Notes

The authors declare no competing financial interest.

■ ACKNOWLEDGMENTS

We thank Isabella Lustrati and Ida Bernabei for their useful collaboration at the synthesis of compounds and Dr. Gilles Pain for critical revision of the manuscript.

■ ABBREVIATION USED

ADME, absorption, distribution, metabolism, and excretion; AIBN, 2,2'-azobis(2-methylpropionitrile), 2-(azo(1-cyano-1-methylethyl))-2-methylpropane nitrile; DCM, dichloromethane; DIPEA, *N*-ethyl-diisopropylamine; DMAP, 4-(*N,N*-dimethylamino) pyridine; DMF, *N,N*-dimethylformamide; DPBS, Dulbecco's phosphate-buffered saline; DTT, dithiothreitol; EDC, *N*-(3-(dimethylamino)propyl)-*N*-ethylcarbodi-

imidehydrochloride; HDAC, histone deacetylase; HNB, hydroxynaphthol blue; pan-HDACis, pan-HDAC inhibitors; PK, pharmacokinetics; PMSE, phenylmethylsulfonyl fluoride; THF, tetrahydrofuran; TFA, trifluoroacetic acid; ZBG, zinc-binding group

■ REFERENCES

- (1) Allfrey, V. G.; Faulkner, R.; Mirsky, A. E. Acetylation and methylation of histones and their possible role in the regulation of RNA synthesis. *Proc. Natl. Acad. Sci. U. S. A.* **1964**, *51*, 786–794.
- (2) Ecker, J.; Witt, O.; Milde, T. Targeting of histone deacetylases in brain tumors. *Future Med.—CNS Oncol.* **2013**, *2*, 359–376.
- (3) Bantscheff, M.; Hopf, C.; Savitski, M. M.; Dittmann, A.; Grandi, P.; Michon, A. M.; Schlegl, J.; Abraham, Y.; Becher, I.; Bergamini, G.; Boesche, M.; Delling, M.; Dümpelfeld, B.; Eberhard, D.; Huthmacher, C.; Mathieson, T.; Poedel, D.; Reader, V.; Strunk, K.; Sweetman, G.; Kruse, U.; Neubauer, G.; Ramsden, N. G.; Drewes, G. Chemo-proteomics profiling of HDAC inhibitors reveals selective targeting of HDAC complexes. *Nature Biotechnol.* **2011**, *29*, 255–265.
- (4) Spiegel, S.; Milstien, S.; Grant, S. Endogenous modulators and pharmacological inhibitors of histone deacetylases in cancer therapy. *Oncogene* **2012**, *31*, 537–551.
- (5) Giannini, G.; Cabri, W.; Fattorusso, C.; Rodriguez, M. HDAC inhibitors in the treatment of cancer: overview and perspectives. *Future Med. Chem.* **2012**, *4*, 1439–1460.
- (6) Zhang, L.; Lei, J.; Shan, Y.; Yang, H.; Ma, Y. Recent Progress in the Development of Histone Deacetylase Inhibitors as Anti-Cancer Agents. *Mini-Rev. Med. Chem.* **2013**, *13*, 1999–2013.
- (7) Wagner, F. F.; Weiwler, M.; Lewis, M. C.; Holson, E. B. Small Molecule Inhibitors of Zinc-dependent Histone Deacetylases. *Neurotherapeutics* **2013**, *10*, 589–604.
- (8) Khan, O.; La Thangue, N. B. HDAC inhibitors in cancer biology: emerging mechanisms and clinical applications. *Immunol. Cell Biol.* **2012**, *90*, 85–94.
- (9) Venugopal, B.; Evans, T. R. Developing histone deacetylase inhibitors as anticancer therapeutics. *Curr. Med. Chem.* **2011**, *18*, 1658–1671.
- (10) Deubzer, H. E.; Schier, M. C.; Oehme, I.; Lodrini, M.; Haendler, B.; Sommer, A.; Witt, O. HDAC11 is a novel drug target in carcinomas. *Int. J. Cancer* **2013**, *132*, 2200–2208.
- (11) Taunton, J.; Collins, J. L.; Schreiber, S. L. Synthesis of Natural and Modified Trapoxins, Useful Reagents for Exploring Histone Deacetylase Function. *J. Am. Chem. Soc.* **1996**, *118*, 10412–10422.
- (12) Thaler, F.; Mercurio, C. Towards Selective Inhibition of Histone Deacetylase Isoforms: What Has Been Achieved, Where We Are and What Will Be Next. *ChemMedChem* **2014**, *9*, 523–536.
- (13) Valente, S.; Mai, A. Small-molecule inhibitors of histone deacetylase for the treatment of cancer and non-cancer diseases: a patent review (2011–2013). *Expert Opin. Ther. Patents* **2014**, *24*, 1–15.
- (14) Grassadonia, A.; Cioffi, P.; Simiele, F.; Iezzi, L.; Zilli, M.; Natoli, C. Role of Hydroxamate-Based Histone Deacetylase Inhibitors (Hb-HDACis) in the Treatment of Solid Malignancies. *Cancers* **2013**, *5*, 919–942.
- (15) Suzuki, T.; Miyata, N. Rational design of non-hydroxamate histone deacetylase inhibitors. *Mini-Rev. Med. Chem.* **2006**, *6*, 515–526.
- (16) Matheson, A. J.; Noble, S. Racecadotril. *Drugs* **2000**, *59*, 829–835 (discussion 836–837).
- (17) Pires de Lima, D. Synthesis of angiotensin-converting enzyme (ACE): an important class of antihypertensive drugs. *Quim. Nova* **1999**, *22*, 375–381.
- (18) Suzuki, T.; Nagano, Y.; Kouketsu, A.; Matsuura, A.; Maruyama, S.; Kurotaki, M.; Nakagawa, H.; Miyata, N. Novel inhibitors of human histone deacetylases: design, synthesis, enzyme inhibition, and cancer cell growth inhibition of SAHA-based non-hydroxamates. *J. Med. Chem.* **2005**, *48*, 1019–1032.

- (19) Suzuki, T.; Kouketsu, A.; Matsuura, A.; Kohara, A.; Ninomiya, S.; Kohda, K.; Miyata, N. Thiol-based SAHA analogues as potent histone deacetylase inhibitors. *Bioorg. Med. Chem. Lett.* **2004**, *14*, 3313–3317.
- (20) Itoh, Y.; Suzuki, T.; Kouketsu, A.; Suzuki, N.; Maeda, S.; Yoshida, M.; Nakagawa, H.; Miyata, N. Design, synthesis, structure–selectivity relationship, and effect on human cancer cells of a novel series of histone deacetylase 6-selective inhibitors. *J. Med. Chem.* **2007**, *50*, 5425–5438.
- (21) Huang, D.; Li, X.; Sun, L.; Xiu, Z.; Nishino, N. Synthesis, evaluation and molecular modeling of cyclic tetrapeptide histone deacetylase inhibitors as anticancer agents. *J. Pept. Sci.* **2012**, *18*, 242–251.
- (22) (a) Breslow, R.; Belvedere, S.; Gershell, L.; Miller, T. A.; Marks, P. A.; Richon, V. M.; Rifkind, R. Class of cytodifferentiating agents and histone deacetylase inhibitors, and methods of use thereof. U.S. Patent 6,511,990-B1, 2003. (b) Breslow, R.; Marks, P. A.; Abhilash, K. G.; Wang, J. Selective HDAC inhibitors. WO 2011146855, 2011. (c) Finnin, M. S.; Donigan, J. R.; Cohen, A.; Richon, V. M.; Rifkind, R. A.; Marks, P. A.; Breslow, R.; Pavletich, N. P. Structures of a histone deacetylase homologue bound to the TSA and SAHA inhibitors. *Nature* **1999**, *401*, 188–193.
- (23) Hanessian, S.; Auzzas, L.; Giannini, G.; Marzi, M.; Cabri, W.; Barbarino, M.; Vesci, L.; Pisano, C. Omega-alkoxy analogues of SAHA (vorinostat) as inhibitors of HDAC: a study of chain-length and stereochemical dependence. *Bioorg. Med. Chem. Lett.* **2007**, *17*, 6261–6265.
- (24) Hanessian, S.; Auzzas, L.; Larsson, A.; Zhang, J.; Giannini, G.; Gallo, G.; Ciacci, A.; Cabri, W. Vorinostat-Like Molecules as Structural, Stereochemical, and Pharmacological Tools. *Med. Chem. Lett.* **2010**, *1*, 70–74.
- (25) Auzzas, L.; Larsson, A.; Matera, R.; Baraldi, A.; Deschenes-Simard, B.; Giannini, G.; Cabri, W.; Battistuzzi, G.; Gallo, G.; Ciacci, A.; Vesci, L.; Pisano, C.; Hanessian, S. Non-natural macrocyclic inhibitors of histone deacetylases: design, synthesis, and activity. *J. Med. Chem.* **2010**, *53*, 8387–8399.
- (26) Taddei, M.; Cini, E.; Giannotti, L.; Giannini, G.; Battistuzzi, G.; Vignola, D.; Vesci, L.; Cabri, W. Lactam based 7-amino suberoylamidehydroxamic acids as potent HDAC inhibitors. *Bioorg. Med. Chem. Lett.* **2014**, *24*, 61–64.
- (27) Witt, D.; Klajn, R.; Barski, P.; Grzybowski, B. A. Applications, Properties and Synthesis of ω -Functionalized *N*-Alkanethiols and Disulfides—The Building Blocks of Self-Assembled Monolayers. *Curr. Org. Chem.* **2004**, *8*, 1763–1797.
- (28) Watanabe, L. A.; Jose, B.; Kato, T.; Nishino, N.; Yoshida, M. Synthesis of L - α -amino- ω - bromoalkanoic acid for side chain modification. *Tetrahedron Lett.* **2004**, *45*, 491–494.
- (29) Zhi, J.; Xiao, Y.; Hu, A. Synthesis of thiol-containing amino acids through alkylation of glycinateketimine. *Synth. Commun.* **2012**, *42*, 914–920.
- (30) Lahm, A.; Paolini, C.; Pallaoro, M.; Nardi, M. C.; Jones, P.; Neddermann, P.; Sambucini, S.; Bottomley, M. J.; Lo Surdo, P.; Carfi, A.; Koch, U.; De Francesco, R.; Steinkühler, C.; Gallinari, P. Unraveling the hidden catalytic activity of vertebrate class IIa histone deacetylases. *Proc. Natl. Acad. Sci. U. S. A.* **2007**, *104*, 17335–17340.
- (31) Yang, X. J.; Gregoire, S. Class II histone deacetylases: from sequence to function, regulation, and clinical implication. *Mol. Cell. Biol.* **2005**, *25*, 2873–2884.
- (32) Vannini, A.; Volpari, C.; Gallinari, P.; Jones, P.; Mattu, M.; Carfi, A.; De Francesco, R.; Steinkühler, C.; Di Marco, S. Substrate binding to histone deacetylases as shown by the crystal structure of the HDAC8–substrate complex. *EMBO Rep.* **2007**, *8*, 879–884.
- (33) Oger, F.; Lecorgne, A.; Sala, E.; Nardese, V.; Demay, F.; Chevance, S.; Desravines, D. C.; Aleksandrova, N.; Le Guével, R.; Lorenzi, S.; Beccari, A. R.; Barath, P.; Hart, D. J.; Bondon, A.; Carettoni, D.; Simonneaux, G.; Salbert, G. Biological and biophysical properties of the histone deacetylase inhibitor suberoylanilidehydroxamic acid are affected by the presence of short alkyl groups on the phenyl ring. *J. Med. Chem.* **2010**, *53*, 1937–1950.
- (34) Somoza, J. R.; Skene, R. J.; Katz, B. A.; Mol, C.; Ho, J. D.; Jennings, A. J.; Luong, C.; Arvai, A.; Buggy, J. J.; Chi, E.; Tang, J.; Sang, B. C.; Vermer, E.; Wynands, R.; Leahy, E. M.; Dougan, D. R.; Snell, G.; Navre, M.; Knuth, M. W.; Swanson, R. V.; McRee, D. E.; Tari, L. W. Structural snapshots of human HDAC8 provide insights into the class I histone deacetylases. *Structure* **2004**, *12*, 1325–1334.
- (35) Strickley, R. G. Solubilizing excipients in oral and injectable formulations. *Pharm. Res.* **2004**, *21*, 201–230.
- (36) HDAC screening was performed by Reaction Biology Corp. (Malvern, PA).
- (37) Skehan, P.; Storeng, R.; Scudiero, D.; Monks, A.; McMahon, J.; Vistica, D.; Warren, J. T.; Bokesch, H.; Kenney, S.; Boyd, M. R. New Colorimetric Cytotoxicity Assay for Anticancer-drug Screening. *J. Natl. Cancer Inst.* **1990**, *82*, 1107–1112.
- (38) *Maestro*, version 9.6; Schrödinger, LLC: New York, 2013.
- (39) *LigPrep*, version 2.8; Schrödinger, LLC: New York, 2013.
- (40) (a) *Schrödinger Suite 2013 Protein Preparation Wizard*; Schrödinger, LLC: New York, 2013; (b) *Epik* version 2.6; Schrödinger, LLC, New York, NY, 2013; (c) *Impact*, version 6.1; Schrödinger, LLC: New York, 2013; (d) *Prime*, version 3.3; Schrödinger, LLC: New York, 2013.
- (41) *Glide*, version 6.1; Schrödinger, LLC: New York, 2013.
- (42) Friesner, R. A.; Banks, J. L.; Murphy, R. B.; Halgren, T. A.; Klicic, J. J.; Mainz, D. T.; Repasky, M. P.; Knoll, E. H.; Shelley, M.; Perry, J. K.; Shaw, D. E.; Francis, P.; Shenkin, P. S. Glide: a new approach for rapid, accurate docking and scoring. 1. Method and assessment of docking accuracy. *J. Med. Chem.* **2004**, *47*, 1739–1749.
- (43) Watson, P. J.; Fairall, L.; Santos, G. M.; Schwabe, J. W. R. Structure of HDAC3 bound to co-repressor and inositol tetrakisphosphate. *Nature* **2012**, *481*, 335–340.
- (44) Vannini, A.; Volpari, C.; Gallinari, P.; Jones, P.; Mattu, M.; Carfi, A.; De Francesco, R.; Steinkühler, C.; Di Marco, S. Substrate binding to histone deacetylases as shown by the crystal structure of the HDAC8–substrate complex. *EMBO Rep.* **2007**, *8*, 879–884.
- (45) Jorgensen, W. L.; Maxwell, D. S.; Tirado-Rives, J. Development and testing of the OPLS all-atom force field on conformational energetics and properties of organic liquids. *J. Am. Chem. Soc.* **1996**, *118*, 11225–11236.
- (46) Cole, K. E.; Dowling, D. P.; Boone, M. A.; Phillips, A. J.; Christianson, D. W. Structural basis of the antiproliferative activity of largazole, a depsipeptide inhibitor of the histone deacetylases. *J. Am. Chem. Soc.* **2011**, *133*, 12474–12477.
- (47) *MacroModel*, version 10.2; Schrödinger, LLC: New York, 2013.
- (48) Dowling, D. P.; Gantt, S. L.; Gattis, S. G.; Fierke, C. A.; Christianson, D. W. Structural studies of human histone deacetylase 8 and its site-specific variants complexed with substrate and inhibitors. *Biochemistry* **2008**, *47*, 13554–13563.
- (49) (a) *Desmond Molecular Dynamics System*, version 3.6, D. E. Shaw Research: New York, 2013; (b) *Maestro-Desmond Interoperability Tools*, version 3.6; Schrödinger: New York, 2013.
- (50) Bowers, K. J.; Chow, E.; Xu, H.; Dror, R. O.; Eastwood, M. P.; Gregerson, B. A.; Klepeis, J. J.; Kolossvary, I.; Moraes, M. A.; Sacerdoti, G. D.; Salmon, J. K.; Shan, Y.; Shaw, D. E. Scalable Algorithms for Molecular Dynamics Simulations on Commodity Clusters, *Proceedings of the ACM/IEEE Conference on Supercomputing (SC06)*, Tampa, FL; Institute of Electrical and Electronics Engineers (IEEE): New York, 2006.
- (51) Feller, S. E.; Zhang, Y.; Pastor, R. W.; Brooks, B. R. Constant pressure molecular dynamics simulation: the Langevin piston method. *J. Chem. Phys.* **1995**, *103*, 4613–4621.
- (52) Lippert, R. A.; Bowers, K. J.; Dror, R. O.; Eastwood, M. P.; Gregersen, B. A.; Klepeis, J. L.; Kolossvary, I.; Shaw, D. E. A common, avoidable source of error in molecular dynamics integrators. *J. Chem. Phys.* **2007**, *126*, 046101.
- (53) Essmann, U.; Perera, L.; Berkowitz, M. L.; Darden, T.; Lee, H.; Pedersen, L. G. A smooth particle mesh ewald method. *J. Chem. Phys.* **1995**, *103*, 8577–8593.
- (54) Tuckerman, M.; Berne, B. J.; Martyna, G. J. Reversible multiple time scale molecular dynamics. *J. Chem. Phys.* **1992**, *97*, 1990–2001.